ASTRONOMY & ASTROPHYSICS
SUPPLEMENT SERIES

Astron. Astrophys. Suppl. Ser. **97**, 851-871 (1993)

Evolutionary sequences of stellar models with semiconvection and convective overshoot. I. $Z = 0.008$

M. Alongi[1,*], G. Bertelli[1,2], A. Bressan[3], C. Chiosi[1], F. Fagotto[1], L. Greggio[4] and E. Nasi[3]

[1] Department of Astronomy, Vicolo Osservatorio 5, 35122 Padua, Italy
[2] National Council of Research, Rome, Italy
[3] Astronomical Observatory, Vicolo Osservatorio 5, 35122 Padua, Italy
[4] Department of Astronomy, Via Zamboni 33, Bologna, 40126 Bologna, Italy

Received December 11, 1991; accepted June 18, 1992

Abstract. — We present two grids of evolutionary stellar models covering the phases of core H- and He-burning for stars having masses in the range $0.6M_{\odot}$ to $100M_{\odot}$ with composition ($Y = 0.25$ and $Z = 0.008$). The computations were performed for two different mixing schemes in the convective regions, i.e. either the classical definition of the convective core during the central H-burning phase and semiconvection during the core He-burning phase or non local overshoot from convective regions all over the major nuclear phases. All the evolutionary models were computed from the main sequence up to the stage of central carbon ignition or to the beginning of the thermally pulsing regime of the asymptotic giant branch phase as appropriate to the value of the initial stellar mass. Massive stars ($M \geq 12M_{\odot}$) were evolved considering the effect of mass loss by stellar wind, whereas low and intermediate mass stars were calculated at constant mass. For these latter, mass loss during the red giant and asymptotic giant branch phases can be easily included following the standard analytical procedure. Care was paid to upgrade the physical input of the numerical code, i.e. nuclear reaction rates and accompanying nucleosynthesis network (16 elements were actually followed), opacities, neutrino energy losses, boundary conditions in the outer layers, and mass loss rates for massive stars. The results are presented in tabular form giving as much information as possible. Finally, we concisely compare the main characteristics of the evolutionary models obtained with the two mixing schemes.

Key words: stars: interiors — stars: evolution — stars: mass loss — nuclear reaction — convection

1. Introduction

The theory of stellar evolution finds applications in many important topics of modern astrophysics such as the understanding of the color-magnitude diagrams (CMD) and luminosity function (LF) of star clusters of any age and chemical composition, the integrated properties of star clusters, the stellar nucleosynthesis, and the chemical and spectral evolution of galaxies.

Each of these topics requires stellar models with accurate and adequate input physics, i.e. nuclear reaction rates, radiative and molecular opacities, mixing in the unstable convective regions, mass loss by stellar wind etc. In addition to this, homogeneity of the physical input and to a less extent of the numerical algorithms used to calculate stellar models is of paramount importance in assessing the reliability of the final result.

Among other points of uncertainty, there is considerable debate at present concerning mixing in stellar interiors. Because a rigorous and fully sound theory of stellar convection is still to be made, the extension of convective regions in real stars is uncertain, and so it is for the physical response to perturbations of the chemical composition in layers that are formally stable according to the classical Schwarzschild condition, $\nabla_R = \nabla_A$, but become convectively unstable as soon as the perturbations are supposed to occur. The complex nature of the mixing processes has been pictured in different ways that resulted into a variety of mixing schemes having different effects on the stellar structure and evolution. See the review by Chiosi et al. (1992a) and the summary discussion below.

As a great deal of evolutionary results depend on the extension of the convective regions, the lack of a generally accepted theory of the extension of convective regions in stellar interiors is critical.

* In memory of Maurizio Alongi who passed away on Wednesday 25 July 1990, in Padova

Extension models can be grouped in two categories: the so-called canonical models in which the extension of convective regions (cores) is based on the use of the Schwarzschild criterion, and those which include the effect of convective overshoot. Recent calculations of canonical models over a wide range of stellar masses and the major nuclear phases of central H- and He-burnings are by Castellani et al. (1990, 1992), which extend the somewhat older grids of VandenBerg (1985), Green et al. (1987), Sweigart et al. (1990).

Models with parameterized descriptions of convective overshoot are by Alongi et al. (1991), Bressan et al. (1981), Bertelli et al. (1985, 1986a,b, 1992a), Bressan et al. (1986), Doom (1982a,b; 1985), Chin & Stothers (1991), Stothers (1985), Stothers & Chin (1990), Matraka et al. (1982), Maeder & Meynet (1987, 1988, 1989, 1991), and Maeder (1990).

Unfortunately the various sets of models neither possessed exactly the same input physics (basically opacity and nuclear rates) nor followed a unique formalism for the extension of the convective regions (both for the classical and the overshoot scheme). Therefore, any conclusion about the adequacy of the adopted mixing scheme and efficiency of convective overshoot was always entangled with a certain degree of ambiguity caused by the lack of homogeneity in the basic physical assumptions.

The impressive amount of CCD photometric data, from which good CMDs and LFs can be obtained, for star clusters and field stars in both the Milky Way and nearby galaxies, the Magellanic Clouds in particular, perhaps makes it possible not only to discriminate among the various mixing schemes but also to constrain the efficiency of convective overshoot, in virtue of the sizable effects that the mixing processes produce on stellar models.

To this aim, we intend to produce large grids of stellar models with homogeneous input physics, different values of the initial chemical composition, and two schemes for treating convective regions, i.e. either the so-called classical scheme or the scheme allowing for non local overshoot. In this paper, the first of the series, we present two large grids of evolutionary models for stars in the mass range $0.6M_{\odot}$ to $100M_{\odot}$. All of the evolutionary sequences were evolved from the zero age main sequence up to the stage of central carbon ignition or to the beginning of the thermally pulsing regime of the asymptotic giant branch (AGB) phase as appropriate to the value of the initial mass. Massive stars ($M \geq 12M_{\odot}$) were computed including also the effect of mass loss by stellar wind all over their entire evolutionary history, whereas low mass and intermediate mass stars were evolved at constant mass. For these latter, the effect of mass loss during the evolution along the red giant branch (RGB) and asymptotic giant branch (AGB) stages can be easily included by means of the standard procedure (see Renzini 1977 and Iben & Renzini 1983 for all details).

Two different mixing schemes were adopted in the model calculations. In the first one, the extension of convective regions is obtained with the canonical Schwarzschild criterion supplemented by the algorithm of semiconvection at the border of the convective He-burning cores (see below). In the second set of models, the extension of the convective regions (cores and envelopes) is fixed by means of a simplified theory of non local overshoot (see below).

The models of massive stars ($12M_{\odot}$ to $100M_{\odot}$) were computed limited to the case of convective overshoot, because on the one hand the effects of the H-semiconvection are known from long time (see Chiosi & Maeder 1986), on the other hand He-semiconvection has virtually no effect in this mass range.

The models of these sets were calculated adopting the chemical composition $Z = 0.008$ and $X = 0.742$, which is most suited to the relatively young population of star clusters in the LMC (Russell & Bessell 1989).

Finally, the stellar models were computed with the Los Alamos Opacity Library (LAOL) of Huebner et al. (1977) leaving aside the new opacity by Iglesias & Rogers (1991a,b). The reason for this choice was that the calculations of our models were almost completed when the new opacity became available. Therefore in order to keep the internal homogeneity of our models, we decided to continue the project with the LAOL. However, in order to evaluate at what extent the new opacity by Iglesias & Rogers (1991a,b), Iglesias et al. (1992), and Rogers & Iglesias (1992) would affect our models, we have calculated two preliminary sequences for a $5M_{\odot}$ star. Because of the low metallicity adopted in these models, and the revision of the iron abundance in the Anders & Grevesse (1989) mixture (Grevesse 1991), the net effect turns out to be small (see the discussion).

2. Mixing in stellar interiors: semiconvection

Hydrogen semiconvection. During the core H-burning phase of massive stars, radiation pressure and electron scattering opacity give rise to a large convective core surrounded by an H-rich region, which is potentially unstable to convection if the original gradient in chemical abundance is left, but stable if suitable mixing is allowed to take place. Theoretical models picture this region of the star to undergo sufficient mixing until the condition of neutrality is restored, but to carry negligible energy flux. The gradient in chemical abundance depends on which condition is used to achieve neutrality, either Schwarzschild or Ledoux. The former condition tends to give smoother chemical profiles and in some cases leads to the onset of a fully intermediate convective layer. It is worth recalling that the Ledoux criterion is a stronger condition favoring stability with respect to the Schwarzschild criterion. Similar instability occurs also during the early shell H-burning

stages. The effects of H-semiconvection on the evolution of massive stars have been summarized by Chiosi & Maeder (1986) and more recently by Chiosi et al. (1992a).

Helium semiconvection. As He-burning proceeds in the convective core of low mass stars in the Horizontal Branch (HB) phase, the C-rich mixture inside the core becomes more opaque than the C-poor material outside and therefore the radiative temperature gradient increases within the core. The resulting superadiabaticity at the edge of the core leads to a progressive increase (local convective overshoot) in the size of the convective core during the early stages of He-burning (Schwarzschild 1970; Paczynski 1971; Castellani et al. 1971a,b). Once the central value of helium falls below $Y_c = 0.7$, the temperature gradient reaches a local minimum, so that continued overshoot is no longer able to restore the neutrality condition at the border of the core. In fact, engulfing fresh helium by local overshoot further decreases the radiative temperature gradient. The core splits into an inner convective core and an outer convective shell. As further helium is captured by the convective shell, this latter tends to become stable, leaving behind a region of varying composition in condition of neutrality ($\nabla_R = \nabla_A$). This zone is called semiconvective. Similar situation occurs in intermediate mass stars once the central helium content has fallen below a certain value. The extension of the semiconvective region varies with the star mass, being important in the low mass and intermediate mass stars up to say 5 $M_\odot$, and negligible in more massive stars. Various algorithms have been devised to treat semiconvection (Castellani et al. 1971b; Demarque & Mengel 1972; Sweigart & Demarque 1972; Gingold 1976; Robertson & Faulkner 1972, Sweigart & Gross 1976, 1978; Castellani et al. 1985; Lattanzio 1986, 1987, 1991; Fagotto 1990). We have followed the scheme of Castellani et al. (1985) according to the revision made by Fagotto (1990). In short, starting from the centre and going outward, the matter in the radiatively stable region above the formal convective core is mixed layer by layer until the neutrality condition is achieved. This picture holds during most of the central He-burning phase.

Breathing convection. As central helium gets as low as $Y_c \simeq 0.1$, the enrichment of fresh helium caused by the semiconvective mixing enhances the rate of energy produced by the 3α reactions in such a way that the radiative gradient at the convective edge is increased, and a very rapid enlargement followed by an equally rapid decrease of the fully convective core takes place (pulse of convection). Several pulses may occur before the complete exhaustion of the central helium content. This convective instability was called breathing convection by Castellani et al. (1985). The net effect is an increase of the core He-burning lifetime τ_{He} and for the models of HB stars a decrease (a factor of 2 to 3) of the ratio R_2 between the AGB and the HB lifetimes with respect to the models where the breathing pulses are suppressed (0.06 instead of 0.15). Because the star counts in globular clusters suggest that $R_2 = 0.15 \pm 0.05$ (Buzzoni et al. 1983), Bressan et al. (1986) concluded that breathing pulses of convection are not likely to occur (see also Caputo et al. 1989). According to Renzini & Fusi-Pecci (1988), while semiconvection is a true theoretical prediction, the breathing pulses are most likely an artifact of the idealized algorithm used to describe mixing (see also Bressan et al. 1986 and Chiosi 1986). It is plausible that the breathing pulses originate from neglecting the possibility of a time dependence in the mixing process. In the light of the above considerations, breathing pulses are suppressed by imposing that the core cannot be enriched in helium by mixing with the outer layers more than a fixed fraction F of the amount burnt by nuclear reactions. By doing this, the time dependence of convection is implicitly taken into account. By imposing that for an HB track of $0.6 M_\odot$ the value of R_2 observed in globular clusters (Buzzoni et al. 1983) is reproduced, we get $F \simeq 1$.

3. Mixing in stellar interiors: overshoot

Motivations: pros and cons. The argument for the occurrence of convective overshoot is that the traditional criteria for convective stability look for the locus where the buoyancy acceleration vanishes. Since it is very plausible that the velocity of the convective elements is not zero at that layer, these will penetrate (overshoot) into regions that are formally stable. If the physical ground of convective overshoot is simple, its formulation and efficiency are much more uncertain. This reflects into the variety of solutions proposed over the years. Compare for instance the contrasting conclusions reached long ago by Saslow & Schwarzschild (1965) and Shaviv & Salpeter (1973). Without going into a long discussion of the topic, we recall a few contributions aimed at introducing a simplified description of penetrative convection suited to stellar model calculations: Maeder (1975), Cloutman & Whitaker (1980), Roxburgh (1978, 1989) Bressan et al. (1981), Xiong (1985, 1986), Kuhfuss (1986), Langer (1986), Baker & Kuhfuss (1987), Zahn (1991), Canuto & Mazzitelli (1991), and Cattaneo et al. (1991).

The resulting overshoot distance at the edge of the convective core greatly differs from one model to another, depending on the assumptions made, going from zero to about 2 H_P (pressure scale height). However, the recent discussion by Zahn (1991) clarifies that under the conditions for nearly adiabatic penetration (amply met in stellar interiors), overshoot above the convective core amounts to a substantial fraction of the core radius, and overshoot at the bottom of a convective envelope is of the order of a pressure scale height. Furthermore, the comparison of extant formulations of overshoot based on the mixing length approach indicates that the formalism

of Bressan et al. (1981) is the one coming closest to results from theoretical studies and numerical simulations of penetrative convection (see Zahn 1991 for more details).

Because a generally accepted theory of convective overshoot is not yet available, and the efficiency of mixing is not well defined recourse has been made to parameterized descriptions, the most simple of which is to specify d/H_P the ratio of the overshoot distance for mixing to the local pressure scale height (e.g. Chin & Stothers 1991; Maeder & Meynet 1987, 1988, 1989; Maeder 1990). Alternatively, more sophisticated formulations are used in which the ratio d/H_P results from the model structure itself (e.g. Maeder 1975; Bressan et al. 1981; Bertelli et al. 1985, 1986). Comparison of stellar models computed with different values of d/H_P (either assumed or calculated) with the observational data is made to infer the overshoot distance.

In the following we will briefly summarize the results of a few studies in which convective overshoot from the core has been amply debated with contrasting appraisal of its extension and efficiency.

Maeder & Mermilliod (1981) analyzing clusters like the Pleiades noticed that the main sequence extends to too bright a luminosity to fit standard models (Brunish & Truran 1982a,b), and suggested a certain amount of overshoot.

Barbaro & Pigatto (1984) noticed that the base of the RGB is populated in clusters older than about $2 - 3\ 10^9$ yr, whereas it is almost missing in clusters with age $1 - 2\ 10^9$ yr as if in this mass range degenerate He-ignition and He-flash were avoided in contrast with classical models. They argued that some overshoot from the convective H-burning cores of stars in the mass range $1.5 - 2.2\ M_\odot$ should occur thus leading to larger core masses and hence to non degenerate core He-ignition.

Aparicio et al. (1990), Bertelli et al. (1992a), Carraro (1991), Carraro et al. (1992), Anthony-Twarog et al. (1991), and Bergbusch et al. (1991), analyzing the morphology of old open clusters, like King 2, IC 4651, NGC 752, NGC 3680, NGC 2243 having turn-off mass in the range $1.5M_\odot$ to $2M_\odot$, seeked to quantify the efficiency of convective overshoot in this mass range. In the light of the discussion below, it is worth recalling that while the models used by Aparicio et al. (1990) were calculated with the Cox & Stewart (1970a,b) opacity, those adopted by Bertelli et al. (1992a), Carraro (1991) and Carraro et al. (1992) were based on the LAOL of Huebner et al. (1977). On the one hand, the studies of Aparicio et al. (1990) and Bertelli et al. (1992a) clarified that the models with overshoot for stars in this mass range calculated by Bertelli et al. (1986a,b) overestimated the overshoot distance (see also the criticism by Renzini 1987), whereas those by Maeder & Meynet (1989, 1991) calculated with a moderate amount of core overshoot suffered from a severe inconsistency in the evaluation of the lifetime. On the other hand they suggested that a certain amount of overshoot is always required. According to the above authors, convective overshoot not exceeding $d/H_P = 0.25$ yield CMDs, LFs, and relative proportions of evolved to main sequence stars, that agree with the observational information. Similar analysis was subsequently performed by Castellani et al. (1992) studying the CMDs of Hyades, Pleiades, Praesepe, NGC 2420, NGC 3680 and NGC 188 with the aid of canonical models and the LAOL. The main conclusion of their study was that if the new opacity is used, there is no need for convective cores significantly larger than those of canonical models and, therefore, convective overshoot is not required. However, in the case of old clusters like NGC 2420 and NGC 188, the analysis of Castellani et al. (1992) is clearly incomplete because the comparison has been made limited to the classical case. As well known, the size of the Schwarzschild convective core decreases with decreasing stellar mass, and so does the total region mixed by overshoot, both eventually recovering the pure radiative structure (see the discussion by Aparicio et al. 1990). Therefore, as shown by Bertelli et al. (1992b), Carraro (1991), and Carraro et al. (1992) using preliminary results of the present calculations, both classical and overshoot models can lead to a reasonable fit of the CMD of old clusters. However, looking both at the CMD and LF, several differencies between the classical and overshoot models can be noticed, which suggest that the latter ought to be preferred (see Carraro et al. 1982 for more details). In the age range of Praesepe, Hyades and Pleiades, where the different mixing schemes may lead to different proportions of stars in main sequence and post main sequence phases, the number of stars beyond the main sequence observed in the CMDS of those clusters is too small to allow any conclusion. As amply discussed by Chiosi et al. (1989a,b), Lattanzio et al. (1991), and Vallenari et al. (1991) on their studies of LMC clusters NGC 1866 and NGC 2164, the formal fit of the CMD without the additional constraint of the LF does not provide sufficient information about the underlying mixing scheme. In fact, while the gross fit of the CMD is always possible independently of the mixing scheme in use, the LFs heavily depend on the evolutionary lifetimes, hence on the mixing scheme. As a matter of fact, the analysis of NGC 1831, whose age is comparable to that of the Hyades but which contains many more stars beyond the main sequence (Vallenari et al. 1992) shows the difficulty encountered by canonical models in matching the CMD and LF at the same time. Owing to their scarcely populated CMDs, Galactic open clusters are poor laboratories to test the subtle implications of convective overshoot. See also the discussion below.

In addition to this, Andersen et al. (1990), Batten et al. (1991), Clausen (1991) and Napiwotzki et al. (1991) explained the position in the CMD of a few stars with well

determined $T_{\rm eff}$'s and gravities with the aid of models with overshoot.

Following the early study by Becker & Mathews (1983), Chiosi et al. (1989a) examined the key LMC cluster NGC 1866 (turn-off mass of about $4 - 5M_{\odot}$) using the photometry obtained by Chiosi et al. (1989b), and insisted on the use of the LF to disentangle canonical from overshoot models. In particular, they showed that the integrated LF of main sequence stars normalized to the number of giants can be a powerful tool to discriminate among different evolutionary scenarios, because it simply reflects the ratio of core H to He-burning lifetimes, strongly affected by the type of mixing in use. In their analysis they assumed as canonical models those calculated by Becker (1981), which were at the base of the study by Becker & Mathews (1983), and as overshoot models those calculated by Bertelli et al. (1985, 1886a,b) with the old Cox & Stewart (1970a,b) opacity. The main result of this study was that substantial overshoot ought to occur in stars with mass of about $5M_{\odot}$. Similar analysis by Brocato & Castellani (1988) and Brocato et al. (1990) led to the opposite conclusion that overshoot from the core is not required if modern opacities are used. Specifically, Brocato et al. (1990) made use of models calculated with the LAOL of Huebner et al. (1977). The same point was also made by Castellani et al. (1992) reviewing the clues for unconventional mixing schemes. However, it was clearly demonstrated by Bressan (1990) that the cause of the agreement with canonical models resided in the different LF for the main sequence stars of NGC 1866 obtained by Brocato et al. (1990) rather than in the use of the "modern opacities". In fact, the opacity alone cannot decrease the ratio of core H- to He-burning below 0.23 while the observations seem to require 0.10. To this purpose see the models of the $5M_{\odot}$ by Alongi et al. (1991) and the case (discussed below) of the $5M_{\odot}$ calculated with the new radiative opacity of Iglesias & Rogers (1991a,b). The reason for the above discrepancy in the LF is not known. It is likely related to the different number of red giants present in the two samples and used in the normalization of the main sequence star LF according to the Chiosi et al. (1989a) method.

The situation with young galactic clusters was discussed in detail by Mermilliod & Maeder (1986) and Maeder & Meynet (1987, 1988, 1989). Similarly, the CMD of Galactic and LMC supergiant stars were examined by Bertelli et al. (1984) and Chiosi et al. (1992a,b). In those studies the conclusion was reached that convective overshoot is needed to explain the properties of the CMDs of those clusters and the relative proportions of supergiant stars of different spectral type. However, Stothers (1991) scrutinizing various tests for the presence of convective overshoot for Galactic stars with masses of $4 - 17M_{\odot}$, members of detached close binary systems or open clusters, and Stothers & Chin (1992) examining the position of the blue supergiants in the CMD of two young rich clusters of the SMC, namely NGC 330 and NGC 458, did not concur to the same conclusion. They argued that core overshoot should not exceed $d/H_{\rm P} = 0.4$ from at least four tests, a tighter upper limit of $d/H_{\rm P} = 0.2$ from the test based on the maximum effective temperature of blue supergiants, and finally that all the best results are formally consistent with the assumption $d/H_{\rm P} = 0$. As a detailed discussion of these studies is beyond the scope of this paper, we will limit ourselves to notice that the test based on the maximum effective temperature of blue supergiants is implicitly based on the assumption that these stars are core He-burners performing a loop in the HRD. Unfortunately, blue loops of bright, hence plausibly massive stars are so sensitive to many physical details (see Chiosi & Maeder 1986 or Chiosi et al. 1992a,b for a general discussion of this topic) that in our view they cannot be safely used to constrain the extension of convective cores. In addition to this, extended loops are possible even in presence of core overshoot if envelope overshoot is allowed to occur (see Alongi et al. 1991 and Chiosi et al. 1992a,b). Furthermore, stars in this mass range are also affected by mass loss both in the blue and red regions of the HRD (see Chiosi & Maeder 1986) so that the effect of core overshoot is certainly entangled with that of stellar winds. However, looking at the handful of supergiant stars shown in the HRD of Fig. 8 of Stothers (1991) we would conclude that models with core overshoot ranging from $d/H_{\rm P} = 0.35$ to $d/H_{\rm P} = 0.70$ are appropriate. Similar arguments apply to the discussion by Stothers & Chin (1992) of the evolved stars in NGC 330 and NGC 458. Finally, Stothers & Chin (1991a) have investigated the combined effect of core overshoot and new radiative opacities (Iglesias & Rogers 1991a,b), compared the model results with the position of a few selected stars in the HRD, and reached identical conclusions.

Other tests for the existence of core overshoot come from the study of the mass discrepancy of cepheid stars. Chiosi et al. (1992c) and Bertelli et al. (1992b) analyzing the CMD and cepheid content of the LMC clusters NGC 2157, NGC 1866 and NGC 2031 showed that the discrepancy between the evolutionary and pulsational mass for classical cepheids does no longer occur if models with overshoot are used. Recently Moskalik et al. (1992) examined the problem of mass discrepancy for the beat and bump cepheids with the aid of the new opacities by Iglesias & Rogers (1991a,b) and Rogers & Iglesias (1992). Compared with the Los Alamos opacity, the period ratios P_1/P_0 and P_2/P_0 are significantly smaller and more sensitive to luminosity and metallicity. For beat cepheids the period ratios P_1/P_0 yield masses that are in better agreement with other determinations. The masses of the bump cepheids are also increased and the mass discrepancy problem is greatly reduced although not completely eliminated. Even if the mass-luminosity relation (MLR)

of classical models is at the base of their analysis, Moskalik et al. (1992) also analyzed the effect of MLR based on overshoot models, in particular the one presented by Chiosi (1989). They find that in the case of beat cepheids the combined effect of the new opacity and overshoot would reduce both the pulsational and evolutionary mass, while in the case of bump cepheids the masses obtained with the new opacity are still smaller than the evolutionary masses obtained from the classical MLR but are compatible with those obtained from overshoot models. Unfortunately the MLR for overshoot models given by Chiosi (1989) is based on models calculated with the old opacity, and complete sets of models with overshoot and new opacity are not yet available, while models with the classical mixing scheme and the new opacity can be found in Stothers & Chin (1991a). These authors argue that the new opacity completely solves the mass discrepancy problem and thus eliminates the need of core overshoot to raise the stellar luminosity.

In addition to the convective core, overshoot may occur at the bottom of the convective envelope during the various phases in which this develops.

The effect of envelope overshoot on stellar models of low and intermediate mass stars has been studied by Alongi et al. (1991), whereas that for high mass stars by Stothers & Chin (1991b) and Chiosi et al. (1992b). Major advantages with envelope overshoot are the reappearance of extended loops during the central He-burning phase compared to models in which core overshoot alone was allowed to occur (Alongi et al. 1991), and the fainter luminosity of the bump in the LF of RGB stars of globular clusters in agreement with the observations (Fusi-Pecci et al. 1990).

Finally, it is worth recalling that overshoot from the core during the central H-burning phase can obviously occur only in stars whose mass is above a certain value, thereinafter referred to as $M_{\rm con}$. In stars lighter than this limit, the central H-burning phase occurs in radiative conditions so that the problem of convective overshoot from the core does not occur. This limiting mass is about $1.0M_{\odot}$ depending on the chemical composition.

What we learn from the above summary is that the question of core overshoot is still far from being settled and that more work is needed to ascertain whether real stars experience significant convective overshoot.

Prescription for core overshoot. The treatment of core overshoot used in these model calculations is based on the formalism developed by Bressan et al. (1981), which stands on the mixing length theory of convection and expresses the overshoot distance by means of $\Lambda \times H_{\rm P}$, where the mixing length parameter Λ is fixed by comparing the models results with the observations. In order to distinguish core overshoot from envelope overshoot, thereinafter we will indicate with $\Lambda_{\rm c}$ the parameter Λ referred to the core, and with $\Lambda_{\rm e}$ the parameter Λ referred to the envelope. Not necessarily the two values of Λ must coincide.

The studies cited above indicated that a unique choice for $\Lambda_{\rm c}$ was not possible over the mass range $0.6M_{\odot}$ to $100M_{\odot}$. The suggestion arose that Λ ought to vary with the initial mass of the star. Therefore, we have made the following assumptions:

i) For models burning hydrogen in the core, the observations are matched when $\Lambda_{\rm c}$ is assumed to be

$$\begin{aligned} &\text{range } 1.0\ M_{\odot}-1.5\ M_{\odot} \quad \Lambda_{\rm c}=0.25\\ &\text{range } 1.6\ M_{\odot}-\ 20\ M_{\odot} \quad \Lambda_{\rm c}=0.50\\ &\text{range } 30\ M_{\odot}-100\ M_{\odot} \quad \Lambda_{\rm c}=1.0 \end{aligned}$$

Specifically, the choice of $\Lambda_{\rm c}=0.25$ in the mass range $1.0M_{\odot}$ to $1.5M_{\odot}$ was motivated by the observational hints examined in the studies by Aparicio et al. (1990), Bertelli et al. (1992a), Carraro (1991), and Carraro et al. (1992). It reflects the fact that in low mass stars a distance as small as $0.5 \times H_{\rm P}$ actually contains a large fraction of the star mass, so that under the action of overshoot the final convective core is several times larger than the original one. A situation which is hard to justify from a physical point of view. We would like to recall that the models for low mass stars calculated by Bertelli et al. (1986a), in which a unique value of $\Lambda_{\rm c}=1$ was adopted all over the mass range from $1.2M_{\odot}$ to $9M_{\odot}$, the convective core during the core H-burning phase of stars with mass in the range $1.2M_{\odot}$ to $1.6M_{\odot}$ enormously exceeded the original one (see also Renzini 1987 for a criticism). The present models supersede the old ones. The choice for the mass range $1.6M_{\odot}$ to $20M_{\odot}$ was based on the study by Chiosi et al. (1989a) and Alongi et al. (1991) of the properties of star clusters in LMC with turnoff masses at about $(4-5)M_{\odot}$, whereas that for the mass range $30M_{\odot}$ to $100M_{\odot}$ was supported by the analysis of the properties of supergiant stars in LMC (Chiosi et al. 1992a,b).

ii) For the core He-burning phase of intermediate and high mass stars, i.e. those igniting helium in the core quietly ($M \geq 1.8M_{\odot}$ in our models with overshoot) the same value of $\Lambda_{\rm c}$ used in the central H-burning phase was adopted, whereas for low mass stars in the HB phase (initial mass in the range $0.6M_{\odot}$ to $1.7M_{\odot}$) the value of $\Lambda_{\rm c}=0.50$ was considered. Once again these choices are basically motivated by the comparison of model results with observations, i.e. the LMC supergiants for the massive stars, the LMC clusters for the intermediate mass stars, and the star counts (the R_2 ratio) for the low mass stars.

However, convective overshoot from the He-burning cores of HB stars demands further discussion. Many preliminary calculations of models in this phase show that in spite of the occurrence of non local overshoot, at the border of the core a semiconvective-like region appears, which is separated from the inner core by a very thin radiative zone. This unusual situation has been pictured

in the following way: complete mixing up to the layer determined by the non local overshoot scheme and semiconvective mixing outside, whose extension is obtained by an algorithm similar to that used for pure semiconvection (Fagotto 1990).

The comparison of these models with those calculated using the classical semiconvective scheme shows that the total size of the region interested by mixing (full and semiconvective) does not depend on the particular algorithm in use (either overshoot plus semiconvection or semiconvection alone). This obviously reflects onto identical lifetimes. Finally, even in occurrence of non local overshoot, the final stages of central He-burning are characterized by the appearance of a few breathing pulses of convection, which however have been suppressed on the basis of the same arguments brought for the purely semiconvective case.

Prescription for envelope overshoot. According to Alongi et al. (1991) the efficiency of envelope overshoot is well represented by an overshoot distance below the classical boundary of the Schwarzschil condition corresponding to $l = \Lambda_e \times H_P$, with $\Lambda_e = 0.7$. This value was adopted in the present models.

4. Input physics and computational details

4.1. *Chemical network, nuclear reaction rates, neutrino losses*

Changes in the chemical abundances were followed in detail using an updated version of the code developed by Greggio (1984), which contains a network of nuclear reactions involving sixteen elements. These are ^{1}H, ^{2}H, ^{3}He, ^{4}He, ^{7}Be, ^{7}Li, ^{12}C, ^{13}C, ^{14}N, ^{16}O, ^{17}O, ^{18}O, ^{20}Ne, ^{22}Ne, ^{25}Mg, and ^{26}Mg.

For the H-burning reactions, the three pp chains and CNO tri-cycle were considered (cf. Maeder 1983), while the following reactions were taken into account during He-burning:

$$^4\mathrm{He}(\alpha,\gamma)^8\mathrm{Be}(\alpha,\gamma)^{12}\mathrm{C}(\alpha,\gamma)^{16}\mathrm{O}(\alpha,\gamma)^{20}\mathrm{Ne}$$
$$(\alpha,\gamma)^{26}\mathrm{Mg}$$
$$^{14}\mathrm{N}(\alpha,\gamma)^{18}\mathrm{F}(\mathrm{e}+\nu)^{18}\mathrm{O}(\alpha,\gamma)^{22}\mathrm{Ne}$$
$$(\alpha,n)^{25}\mathrm{Mg}$$

The reaction rates were taken from Caughlan & Fowler (1988). In particular, the rate for the ^{12}C$(\alpha,\gamma)^{16}$O reaction is somewhat lower than the value estimated by Kettner et al. (1982), Langanke & Koonin (1982), and Caughlan et al. (1985) and it is almost similar to the value given by Fowler et al. (1975).

The β-decay processes and the ^{8}Be$(\alpha,\gamma)^{12}$C reaction were considered to take place instantaneously. Finally, the screening factors were derived from Graboske et al. (1973).

The abundances of the light elements such as ^{2}H, ^{7}Be and ^{7}Li were considered at the equilibrium (creation rate equal to the destruction rate).

The abundances of the remaining elements ^{1}H, ^{3}He, ^{4}He, ^{12}C, ^{13}C, ^{14}N, ^{16}O, ^{17}O, ^{18}O, ^{20}Ne, ^{22}Ne, ^{25}Mg, ^{26}Mg were followed in detail using an explicit scheme of integration according to the formulation by Arnett & Truran (1969).

Denoting by Y_i the by mass abundance of the elemental species i, $Y_i = X_i/A_i$, where X_i is the mass fraction of the species i and A_i its atomic mass number, the time variations of the abundances are governed by the system of equations below (see also Maeder 1983)

$$\mathrm{d}Y_i/\mathrm{d}t = -[ij]Y_iY_j + [\mathrm{rs}]Y_rY_s \qquad (1)$$

where $[ij]$ is the rate of the generic reaction converting the element i into another element because of the interaction with the element j, whereas [rs] is the rate of the generic reaction transforming elements r and s into the element i.

Because an explicit scheme is adopted, the temporal variation of the abundances is decoupled from the physical structure of the models, i.e. the reaction rates are calculated at given temperature and density of the models at each evolutionary time step Δt. The system of differential Eqs (1) is integrated over the evolutionary time interval (Δt), determined on the basis of the structural variations of the stellar models, by means of mini time steps (δt), whose number depends on the temperature in the given mesh point, if convectively stable. In convective regions, instead, the length of the mini time step δt is controlled by the difference in the results obtained with one integration over the whole Δt, and that obtained with two successive integrations over $(\Delta t)/2$. In order to save computational time, the variations of the abundances in convective regions are determined from the mean rates, averaged over the whole region, as in Iben (1964). The variations of the abundance of a species i is determined by

$$\Delta Y_i = (\mathrm{d}Y_i/\mathrm{d}t)\,.(\Delta t), \qquad (2)$$

where the derivatives are computed evaluating the reaction rates at $t + (\Delta t)/2$, by means of extrapolation from the two preceeding models. During H-burning, special care has been paid to avoid oscillations in the abundances once equilibrium between supplying and depleting reactions is achieved by any element: the results of the numerical integration are compared to the appropriate equilibrium abundances at each time step, and the equilibrium value is adopted if necessary. The conservations of the total number of CNO nuclei and of the total number of nucleons are secured in the computation of the abundances of ^{14}N and ^{3}He, respectively, once equilibrium of these two elements is achieved.

Finally, the rates of neutrino emissions are from Munakata et al. (1985).

4.2. *Radiative, conductive, and molecular opacities*

Radiative and conductive opacities were taken from the LAOL of Huebner et al. (1977) for temperatures up to $T \geq 10^4$ K. For lower temperatures, the opacity was derived from the tables of Cox & Stewart (1970a,b). The values of the opacity were obtained by bicubic spline interpolations in temperature and density among tables with different chemical composition. A linear interpolation between neighbouring tables accounts for the effect of the current chemical abundances. The contribution to the opacity CN, CO, H_2O and TiO molecules was included by means of the analitical relationships by Bessel et al. (1989, 1991). These are based on the opacity tables including molecular sources computed by Alexander (1975) & Alexander et al. (1983).

Recently the LAOL of Huebner et al. (1977) has been superseeded by the new radiative opacities of Iglesias et al. (1987, 1990) and Iglesias & Rogers (1991a,b). These opacities differ from the LAOL in the mid temperature region $10^5 \leq T \leq 10^6$K where significant increase (bump-like structure) is found centered at about Log $T \simeq 5.3$. With respect to the classical LAOL, the new opacity is increased by a factor which depends on the chemical composition, being about 3.5 for solar metallicity and lower and lower as the metallicity tends to zero. However, as the grid of models presented in this paper were almost completed when the new opacity tables became available to us, we decided to complete the project with the LAOL. However, two sequences for a $5M_\odot$ star with different metallicities were computed to evaluate the effect of the new opacity with respect to the old one. The results are presented below.

4.3. *Outermost convection*

Convection in the outermost envelope was treated with the mixing length theory to derive thereby the temperature gradient. The mixing length parameter was assumed to be 1.5 H_p. VandenBerg (1991) discussed the effects of changing the mixing length parameter on the morphology of the evolutionary track in the HR Diagram (HRD), and stressed the importance of its calibration on some observables. The value we have adopted is constrained by imposing that the $1M_\odot$ star with chemical composition $Z = 0.017$, $Y = 0.27$ and age of 4.6 10^9 yr matches the luminosity, effective temperature, and radius of the Sun.

It is worth noticing that the differences in the adopted value of the mixing length parameter that are known to exist among different authors, simply reflect differences in treatment of the outermost layers (opacity, $T(\tau)$ relation in the atmosphere, etc). However, provided that the mixing length is calibrated on some observational constraints, the stellar models are at least internally consistent if not fully equivalent.

4.4. *Other computational details*

Shift of the H-burning shell. In order to speed up the numerical computations of models of low mass stars climbing along the RGB, the thin H-burning shell in the RGB models was artificially shifted outward following the prescription by Harm & Schwarzschild (1966).

Initial models of HB. Since a detailed calculation of the He-flash was beyond the aims of this paper, the calculation of models at the RGB tip were interrupted when the central energy output during the He-flash was about one hundred times the model luminosity. Models of a fictitious Zero Age Horizontal Branch (ZAHB) were constructed using the core mass, surface abundances, physical structure in the inner layers (location of the thin H-burning shell), and envelope mass pertaining to a star at the tip of the RGB. The major differences are in the central composition which takes into account the incipient central mixing and consumption of central helium abundance that occurred during the He-flash stage (see Iben & Renzini 1984; Renzini & Fusi-Pecci 1988 for all details and referencing), and removal of electron degeneracy in the core. The decrease in central helium abundance following the He-flash has been assumed to be the same in all the ZAHB models ($\Delta Y = 0.05$). Mass loss by stellar wind during the RGB phase (see Renzini 1977), which would decrease the envelope mass of our ZAHB models with respect to the initial value, is not included in the tabulated models (see below). This is less of a problem because the real mass of ZAHB stars can be easily obtained by assuming a particular algorithm for the mass loss rates, by scaling the envelope mass to the new value, and by interpolating among the tabulated models. It is worth recalling that the core masses of these stars are nearly indentical because they reflect the convergency of the electron degenerate helium cores during the RGB phase to a common value (see Iben 1991 for all details).

Mass zoning and time steps. The mass zoning in the stellar models as well as the adopted time step between two successive models depend from the underlying evolutionary phase. The higher the desired numerical accuracy or the steeper the physical and chemical gradients across the model structure, the higher is the number of mesh points, and the shorter is the time step.

4.5. *Model of massive stars* ($M \geq 12M_\odot$)

The models of stars more massive than $12M_\odot$ were computed with slightly different physical input and limited to the case of convective overshoot. They differ from those of lower mass for the radiative opacity, the inclusion of mass loss all over the entire evolutionary history, and the existence of a pronounced density inversion in the outermost layers.

Radiative opacities. Long ago Bertelli et al. (1984) proposed models of massive stars aimed at explaining the overall properties of the CMD of supergiant stars in the Milky Way and LMC, in which the radiative opacities where supposed to show a bump-like structure in the mid temperature region similar to that found by Iglesias & Rogers (1991a,b) in their modern opacity calculations. The opacity bump was centered at about Log $T \simeq 5.8$. In order to evaluate at what extent the new opacities would affect the results of Bertelli et al. (1984) without changing the main opacity library, we have artificially introduced a bump-like structure in the LAOL according to the formalism of Bertelli et al. (1984) and imposed that the results by Iglesias et al. (1987, 1990) and Iglesias & Rogers (1991a,b) are matched. This modification in the opacity is limited to stars in the mass range $30M_{\odot} \leq M \leq 100M_{\odot}$. Because the opacity increase in the Iglesias et al. (1987, 1990) and Iglesias & Rogers (1991a,b) calculations occurs at temperatures somewhat lower than in Bertelli et al. (1984), it is an easy matter to understand that their effect on stellar models will be much less important than in the calculations by Bertelli et al. (1984).

Mass loss. The evolution of massive stars is dominated by mass loss by stellar wind (see Chiosi & Maeder 1986; Chiosi et al. 1992a,b). In the present calculations we adopted the empirical formulation of the mass loss rate by de Jager et al. (1988) for all evolutionary stages from the main sequence up to the so-called de Jager limit in the CMD. Beyond this limit, the mass loss rate was increased to $10^{-3}\ M_{\odot}\ \mathrm{yr}^{-1}$ as suggested by the observational data for the Luminous Blue Variables (LBV), and it followed the Langer (1989) prescription for the WR stages. We assumed that a star reaches the WR stage when the surface abundance of hydrogen falls below $X = 0.300$.

Density inversion. In the outermost layers of stars with $T_{\rm eff} \leq 10^4$K a convective zone appears caused by the incomplete ionization of hydrogen. In massive stars this zone develops early on in the evolution, while they are crossing the CMD from the main sequence to the red supergiant region.

If convection is treated according to the mixing-length theory with the mixing-length proportional to the pressure scale height, $l = \alpha \times H_{\rm P}$, and the parameter α in the range (1-2), when $T_{\rm eff} \leq 10^4$K a density inversion occurs, i.e. the density reaches a minimum and then starts to increase at increasing radius. This situation is probably unphysical, and it has been the subject of many speculations, e.g. whether it can cause a sudden increase of the mass loss rate, or lead to the Rayleigh-Taylor instability, etc. In addition to this, since the existence of a strong negative gradient in the density can cause numerical difficulties in calculating stellar models, the problem has been often avoided by adopting the density scale height H_{ρ} instead of $H_{\rm P}$ in the mixing length theory. As expected, the density inversion is eliminated because the external convection becomes much more efficient and the actual temperature gradient gets close to the adiabatic value. In our calculations, we have imposed that the density inversion cannot develop by assuming that the temperature gradient $\nabla_{\rm T}$ is such that the density gradient obeys the condition $\nabla_{\rho} \geq 0$. The required temperature gradient is given by $\nabla_{T_{\max}} = \dfrac{1 - \chi_{\mu}\nabla_{\mu}}{\chi_T}$, where ∇_{μ} is the gradient in molecular weight, and χ_{μ} and χ_T have the usual meaning.

5. Evolutionary results

The results of model calculations are presented in Tables 1 to 8 organized as a function of the mixing scheme, the physical conditions at the stage of core He-ignition (either He-flash or quiet He-burning), and the evolutionary phase. The results for models undergoing He-flash are presented separately for the stages from the main sequence to the tip of the RGB and the stages from quiet He-burning (HB) to the start of the thermally pulsing regime of the AGB phase (TPAGB). The stages from core He-exhaustion to the start of TPAGB regime are otherwise indicated as early AGB (EAGB). The results for models igniting helium in the core quietly are given in a unique table from the main sequence to the start of the TPAGB (intermediate mass stars) or central C-ignition (massive stars). The layout of the tables takes into account the effect of the mixing scheme on the value for the transition masses $M_{\rm HeF}$ and $M_{\rm up}$ (see below).

The legend of all tables is as follows:

AGE	:	age of models in years
$L/L_{\odot}$	:	logarithm (base 10) of the total luminosity in solar units
$T_{\rm eff}$	:	logarithm (base 10) of the effective temperature
G	:	logarithm (base 10) of the surface gravity
$T_{\rm c}$	:	logarithm (base 10) of the central temperature
$\rho_{\rm c}$	:	logarithm (base 10) of the central density
COMP	:	central abundance (by mass) of hydrogen or helium
$X_{\rm C}$	:	central abundance of ^{12}C
$X_{\rm O}$	:	central abundance of ^{16}O
$Conv$	:	fractionary mass of the convective core
$Q_{\rm disc}$	:	fractionary mass of the firts mesh point where the chemical composition differs from the surface value
$L_{\rm H}$	:	logarithm (base 10) of the hydrogen luminosity in solar units
$Q1_{\rm H}$	:	fractionary mass of the inner border of the hydrogen rich region
$Q2_{\rm H}$	:	fractionary mass of the outer border of the H-burning region. The boundary is taken where the nuclear energy generation rate becomes greater than a suitable value

L_{He} : logarithm (base 10) of the helium luminosity in solar units
$Q1_{He}$: fractionary mass of the inner border of the He-burning region (when greater than zero He-burning is in a shell). The boundary is taken where the nuclear energy generation rate becomes greater than a suitable value
$Q2_{He}$: fractionary mass of the upper border of the He-burning region. The boundary is taken as above
L_C logarithm (base 10) of the carbon luminosity in solar units
L_ν : logarithm (base 10) of the neutrinos luminosity (absolute value) in solar units
$Q_{T_{max}}$: fractionary mass of the point where the temperature attains the maximum value
M_{dot} : logarithm (base 10) of the absolute value of the mass loss rate in solar masses per year
X_{sur} : surface abundance (by mass) of hydrogen
Y_{sur} : surface abundance (by mass) of helium
XC_{sur} : surface abundance (by mass) of carbon
XN_{sur} : surface abundance (by mass) of nytrogen
XO_{sur} : surface abundance (by mass) of oxygen

5.1. *Models with semiconvection*

Table 1 summarizes the results from the main sequence to the tip of the RGB for models with mass in the range $0.6M_\odot \leq M \leq M_{HeF}$ calculated according to the classical scheme. This means that for stars more massive than M_{con} the dimension of the convective core during the central H-burning phase and the extension of the convective envelope along the RGB are determined by the Schwarzschild condition $\nabla_R = \nabla_A$. For stars lighter than M_{con} the central H-burning is radiative, whereas the envelope convection along the RGB follows the above criterion. With the adopted chemical composition M_{con} is $0.9M_\odot$. As known since long time, M_{HeF} is about $2.1M_\odot$ (Iben & Renzini 1983). However, there is some uncertainty in defining M_{He} because the transition between the two regimes takes place over a finite mass interval (Bertelli et al. 1986a; Sweigart et al. 1990).

Table 2 contains the results for the core He-burning and EAGB phases for the models of Table 1 calculated according to the semiconvective mixing. The star masses go from $0.6M_\odot$ to $2.1M_\odot$. Core He-burning occurs in either HB or clump depending on the stellar mass. Mass loss by stellar wind during the RGB phase can be easily incorporated to determine the real mass of the stars during the central He-burning phase. The tabulated values of the stellar mass encompass all possible cases for the present chemical composition.

Finally, Table 3 summarizes the results for stars in the range $2.2M_\odot$ to $9M_\odot$ from the main sequence to the start of the TPAGB phase or central C-ignition in non degenerate conditions. It is worth recalling that stars in this mass range avoid core He-flash. With the adopted chemical composition M_{up} is between $7M_\odot$ and $8M_\odot$ (see also Iben & Renzini 1983).

5.2. *Models with convective overshoot*

Table 4 contains the data for the stars in the mass range $0.6M_\odot \leq M \leq 1.7M_\odot$ up to the tip of the RGB calculated with the overshoot scheme. Like in the classical scheme, stars lighter than M_{con} are affected by mixing only during the RGB phase. With respect to the results obtained with the classical scheme, the surface abundances at the first dredge-up and the luminosity of the stage at which the H-burning shell crosses the discontinuity in the chemical profile are changed by the envelope overshoot (see below). On the contrary, stars more massive than M_{con} are significantly affected by the different mixing scheme in both the central H-burning and RGB phases. The models of Table 4 undergo core He-flash but, because of overshoot (see below for more details), the limiting mass M_{HeF} is now $1.7M_\odot$. The same uncertainty in the definition of M_{HeF} encountered with the semiconvective models still exists with the overshoot models.

We have already pointed out that in models undergoing core He-flash, the core He-burning phase must obey the constraint that the lifetime and hence mass size of the convective core, match the observational ratio of star counts R_2. This means that independently of the mixing scheme, the model structure of He-burning stars must be the same. It follows that models calculated with convective overshoot should possess the same size of the mixed central region as in models calculated with semiconvection. The choice made for Λ_c provides such an agreement. This is shown by the results presented in Figs. 1 and 2, where the central helium content Y_c is plotted as a function of the lifetime during the core He-burning phases of model stars of $0.6M_\odot$ and $1.5M_\odot$, respectively, calculated with both the semiconvective and the overshoot scheme. The evolutionary tracks in the HRD are virtually undistinguishable one from the others. Therefore, the models of Table 2 calculated with semiconvection are also representative of the results that one would obtain with the overshoot scheme. This strictly holds for the models in core He-burning phase whose mass is in the range $0.6M_\odot$ to $1.5M_\odot$. In spite of the convergency of all model stars to a common M_{He} core during the RGB phase in this mass range, stars slightly more massive than $1.5M_\odot$ are however somewhat more dependent on the mixing scheme adopted during the core H-burning phase and at the tip of the RGB they possess a M_{He} core slightly different from the corresponding one in models calculated according to the classical scheme. Their evolution during the central He-burning phase is therefore slightly different with respect to that of the semiconvective case (Table 2). These

models ($1.6M_\odot$ and $1.7M_\odot$)are displayed in Table 5 together with the stages of EAGB.

Above $1.7M_\odot$, the evolution is entirely dominated by the overshoot scheme. Table 6 describes the evolutionary results from the main sequence to the end of the EAGB for stars in the mass range $1.8M_\odot \leq M \leq 9M_\odot$. With the adopted efficiency of convective overshoot $M_{\rm up}$ is now in the range $5M_\odot$ to $6M_\odot$. Specifically, the $5M_\odot$ star reaches the TPAGB phase and, if evolved at constant mass, it will ignite carbon in highly degenerate conditions (with ensuing deflagration of the core) once the mass of the C-O core has grown to the Chandrasekhar limit of $1.4M_\odot$. On the contrary, the $6M_\odot$ ignites carbon off center and by lifting the electron degeneracy in the C-O core proceeds to quiet C-burning (see also Bertelli et al. 1986a).

Finally, Table 7 contains the results for the evolution of massive stars ($12M_\odot \leq M \leq 100M_\odot$). The layout of Table 7 is somewhat different from the one used in the previous tables. The displayed models go from the main sequence to the stage of central C-ignition.

6. Properties of the stellar models

As the effects of both semiconvection and overshoot on stellar models are known since long time (see Chiosi et al. 1992a,b recent reviews of this topic), the discussion below will be kept very short. However, we would like to emphasize that previous comparisons of the results from the semiconvective scheme with those from the overshoot scheme were always biased by the fact that evolutionary models calculated by different authors were used. Those models, although similar each other within a given mixing scheme, often differed in the input physics (opacities, nuclear reaction rates, the $^{12}C(\alpha,\gamma)^{16}O$ in particular, the algorithm used to follow the temporal evolution of chemical elements, and many other both physical and computational details). The net effect of adopting a different mixing scheme was therefore difficult to single out. In virtue of their homogeneity, the present models offer a unique opportunity.

We start presenting the evolutionary path in the HRD for the models given in Tables 1 to 7. Specifically, Fig. 3 refers to the semiconvective models and shows the evolutionary tracks up to the tip of the RGB for the stars undergoing He-flash (low mass stars) and to the start of the TPAGB for the others. The HRD for the stages from quiet core He-burning to the start of the TPAGB for the low mass stars of this type of models is shown in Fig. 4. Figure 5 shows the same as in Fig. 3 but for models with overshoot including the range of massive stars. The HRD of the low mass range for the overshoot models is identical to that for the semiconvective models already shown in Fig. 4.

6.1. *Core and shell H-burning phases*

Models with overshoot possess more massive convective cores, run at higher luminosities and live longer than classical models. They also extend the main sequence band over a wider range of $T_{\rm eff}$s (compare Figs. 3 and 5). In Table 8 we summarize the lifetimes for the core H- and He-burning, $\tau_{\rm H}$, and $\tau_{\rm He}$ respectively, the ratio $\tau_{\rm He}/\tau_{\rm H}$, and the ratio of the EAGB lifetime to the He-burning lifetime, $\tau_{\rm EAGB}/\tau_{\rm He}$ (this latter given only when the EAGB phase occurs) as a function of the initial mass of the star for the semiconvective and overshoot models. Finally, in the same table we also give the ratios of the core H-burning and core He-burning lifetimes of models with overshoot to those of models with semiconvection. These ratios are indicated $(\tau_{\rm H})_{\rm ov}/(\tau_{\rm H})_{\rm se}$ and $(\tau_{\rm He})_{\rm ov}/(\tau_{\rm He})_{\rm se}$, respectively. At increasing mass of the star, the ratio $\tau_{\rm He}/\tau_{\rm H}$ increases from the low value typical of globular cluster stars to a maximum value in correspondence of a certain value of the mass which depends on the mixing scheme, i.e. $2M_\odot$ for overshoot models and $2.5M_\odot$ for classical model with semiconvection, and then decreases again. The ratio $(\tau_{\rm H})_{\rm ov}/(\tau_{\rm H})_{\rm se}$, is obviously one for $M \leq 0.9M_\odot$, increases to about 1.2 in the mass range $1.2M_\odot$ to $1.5M_\odot$, raises to a maximum (1.34) at $1.6M_\odot$, because of the different value for $\Lambda_{\rm c}$ adopted for stars above $1.5M_\odot$, and then smoothly declines toward the value of 1.23 for the $9M_\odot$. In short, the ratio $(\tau_{\rm H})_{\rm ov}/(\tau_{\rm H})_{\rm se}$ is confined between 1.23 and 1.34 for stars in the mass range $1.2M_\odot$ to $9M_\odot$. The gradual decline is caused by the gradual per cent decrease in the growth by overshoot of the mass of the convective core (and hence mass of the helium core at the end of the H-burning phase), which determines a per cent decrease in the H-burning lifetime. Finally, it is worth noticing the non monotonic behaviour of the lifetime ratio $(\tau_{\rm He})_{\rm ov}/(\tau_{\rm He})_{\rm se}$, which first increases with the star mass, raises to the maximum value of 2.9 at about $1.8M_\odot$, and then decreases to about 0.5 for more massive stars. This can be understood as the result of the overwhelming importance of the higher luminosity in models with overshoot. Specifically, while in the lower mass range, the increase in the core mass by overshoot dominates and therefore prolonges the core He-burning lifetimes, in the upper mass range the increase in the luminosity is not compensated by the increase in the core mass, and the core He-burning lifetime actually gets shorter than in models with the classical mixing scheme. It goes without saying that the above trends are more and more pronounced at increasing $\Lambda_{\rm c}$.

6.2. *Core He-burning phase*

The overluminosity caused by overshooting during the core H-burning phase still remains during the core He-burning phases for stars with initial mass greater than $M_{\rm HeF}$. The mass of the H-exhausted core, $M_{\rm He}$, and the mass of the He-burning convective core are increased un-

der the action of convective overshoot. As a consequence of the higher luminosity, the lifetime of the He-burning phase gets shorter in spite of the increase in the core mass: the ratio $(\tau_{He})_{ov}/(\tau_{He})_{se}$ is about 0.5 in the range $3M_{\odot}$ to $5M_{\odot}$, then increases up to 0.63 as the mass increases to $9M_{\odot}$. In general the ratio τ_{He}/τ_{H} increases up to the transition mass M_{HeF}, then it tends to decrease. In the mass range $2M_{\odot}$ to $9M_{\odot}$ the ratio τ_{He}/τ_{H} for semiconvective models is approximately 2-3 times larger than for models with overshoot. This simply reflects the shorter duration of the core He-burning phase caused by the overluminosity in models with core overshoot. The maximum difference occurs for stars with mass in the range $2M_{\odot}$ to $3M_{\odot}$. The observational implication is very important, as this result will change our expectation for the relative number of post main sequence versus main sequence stars. It follows from this that star clusters with turnoff mass in the above range are the best suited candidates to discriminate between the two mixing schemes.

Table 9 contains a few relevant quantities that bear on the interpretation of the CMD of star clusters and supergiant stars. The evolutionary tracks of stars with mass from $3M_{\odot}$ up to about $20M_{\odot}$ are characterized by loops in the CMD taking place during the core He-burning phase. In lighter stars, the core He-burning phase occurs in either the HB or the clump as appropriate to the star mass, whereas in stars more massive than $20M_{\odot}$ the loop is destroyed by the overwhelming effect of mass loss. In the mass range where the loop can develop, its extension depends on the star mass, chemical composition, and mixing scheme. In short, the loops get wider at increasing mass and decreasing metallicity. As far as the mixing scheme is concerned, at given mass and metallicity, classical models with semiconvection usually exhibit extended loops, whereas models with core overshoot alone possess much less extended loops (see Bertelli et al. 1985). This constituted a drawback of overshoot models when used to explain the CMD of intermediate age clusters (see Chiosi et al. 1989a,b). Specifically, this type of models that otherwise could easily account for the relative number of post main sequence to main sequence stars, always found it difficult to match the observed distribution of giant stars as a function of T_{eff} (color). The disagreement was removed by Alongi et al. (1991) by invoking in models with core overshoot, the concomitant occurrence of envelope overshoot. Extended loops were back again. This is visible from data summarized in Table 9. They are Log $L/L_{\odot}$ and T_{eff} of the hottest point in the loops, the lifetime ratio τ_{He}/τ_{H}, and an annotation identifying the input physics. For overshoot models, the parameters Λ of the internal and external overshoot are also specified. Looking at the extension of the loops in the CMD, we notice that in models with overshoot they are as large as or even larger than those of classical models with semiconvection (e.g. stars with mass comprised between $4M_{\odot}$ and $7M_{\odot}$).

As already mentioned, with respect to the results obtained with the classical mixing scheme, envelope overshoot alters both the surface abundances determined by the firts dredge-up, and the luminosity of the RGB stage at which the H-burning shell reaches the discontinuity in the chemical profile. The variations in the surface abundances are small (see below), whereas the effect on the luminosity of that particular stage is more important. As well known, when the H-burning shell reaches the discontinuity in the chemical profile, the evolutionary rate along the RGB temporarily slows down, and manifests itself as a bump in the luminosity function of the RGB stars. Since envelope overshoot shifts the discontinuity to deeper layers, the H-burning shell reaches the discontinuity early on during the RGB phase, i.e. at lower luminosities. With respect to the classical models, the mean luminosity of the bump is decreased by about Δ Log $L/L_{\odot} = 0.2$ or equivalently by $\Delta M_{bol} = 0.5$. The situation is illustrated in Fig. 6, which displays the bump luminosity as a function of the stars mass for both the classical and overshoot models.

6.3. *Critical masses M_{HeF} and M_{up}*

Confirming previous results (see the discussion in Bertelli et al. 1985 and Chiosi et al. 1991a), in models with overshoot, due to the larger He and C-O cores left over at the end of central H and He-burning phases, both M_{HeF} and M_{up} are lower than in classic models. Although the exact determination of M_{HeF} and M_{up} is beyond the scope of this paper, from the results given in Tables 1 to 6, M_{HeF} is between $1.7M_{\odot}$ and $1.8M_{\odot}$ for overshoot models instead of $2.1M_{\odot}$ to $2.2M_{\odot}$ for classical models with semiconvection. Furthermore, it is also evident that the transition from core He-flash to quiet He-burning does not take place discontinuously, but over a finite mass interval. Similarly, M_{up} falls between $5M_{\odot}$ and $6M_{\odot}$ for overshoot models instead of $7M_{\odot}$ to $8M_{\odot}$ for the classical ones.

6.4. *Evolution of surface abundances*

Nuclear burning in deep layers (shell H- and He-burning regions) and external mixing concur to alter the chemical abundances at the surface of the stars. In this section we present the changes of surface abundances caused by the first and second dredge-up episodes in absence of mass loss. It is worth recalling that the first dredge-up may occur when the stars climb the Hayashi line prior to core He-burning ignition, whereas the second dredge-up may occur in a suitable mass range (see below) of intermediate mass stars prior to the start of the thermally pulsing regime of the AGB phase (TPAGB). The effect of mass loss on the surface abundances can be easily incorporated following the method suggested long ago by Renzini & Voli (1981).

First dredge-up. The changes in surface chemical abundances induced by the first dredge-up are summarized in Tables 10 and 11 for semiconvective and overshoot models, respectively. In these tables we display as function of the star mass the initial abundance (by mass) of the following elements (^{1}H, ^{3}He, ^{4}He, ^{12}C, ^{13}C, ^{14}N, ^{15}N, ^{16}O, ^{17}O, ^{18}O) and their surface abundances after the first dredge-up has occurred. The third column of each table gives the fractionary mass ($Q_{\rm conv}$) of the layer reached by the external convection at its maximum penetration. Finally, the last two columns show the ratios ^{12}C/^{13}C and $(^{14}\mathrm{N})\,/\,(^{14}\mathrm{N})_i$. This latter is the enhancement factor of ^{14}N with respect to the initial value $(^{14}\mathrm{N})_i$. First of all, it is worth noticing that the inclusion of envelope overshoot does not change the value of $Q_{\rm conv}$ by a significant amount. This simply because at the bottom of the envelope over a distance of about $0.7H_{\rm p}$ very little variation in mass corresponds to a large variation in pressure. This is a well known property of stellar models which essentially consist of a compact core and a diluted envelope (see also Alongi et al. 1991 for more details). As a consequence of this, the surface abundances are only modestly affected by the kind of mixing supposed to occur in the outer envelope.

The surface abundances are much more sensitive to the initial mass of the star. Specifically, with respect to the initial value, ^{1}H is decreased by about 3%, whereas ^{4}He is increased by approximately the same amount. ^{12}C and ^{16}O are either constant (low mass end) or decreased by about 10% (upper mass end). Much more conspicuous variations occur for the other elements: ^{3}He goes up by approximately a factor of 80 in the low mass range and of 20 in the upper mass range. ^{13}C and ^{14}N are increased by a factor of about 2, whereas ^{15}N is somewhat decreased. ^{17}O increases with the star mass up to a factor of 10, whereas ^{18}O remains about constant. Furthermore, at increasing star mass the ratio ^{12}C/^{13}C decreases from the value of 82 (initial value 83) for the $0.6M_\odot$ star down to a nearly constant value of 20 starting from about $1.5M_\odot$ up to $9M_\odot$. Finally, ^{14}N increases with the star mass and the ratio $(^{14}\mathrm{N})\,/\,(^{14}\mathrm{N})_i$ goes from 1 for the $0.6M_\odot$ to a value comprised between 2 and 3 for stars in the mass range $1.5M_\odot$ to $9M_\odot$. The abundances of those elements not displayed in Tables 10 and 11 remain constant with respect to their initial value.

Second dredge-up. Similar changes in the surface abundances occur during the second dredge-up when the base of the convective envelope extends down to layers within the H-exhausted core. The effects of the second dredge-up are however limited to masses greater than about $3M_\odot$ and lighter than about $7M_\odot$, as outside this mass range the envelope convection cannot penetrate into the H-exhausted core. In such a case the changes in the surface chemical abundances produced by the second episode of extended envelope convection are negligibly small.

Table 12 summarizes the values of the surface abundances at the end of the second dredge-up for stars in the mass range $3M_\odot$ to $9M_\odot$. The top part of Table 12 refers to classical models with semiconvection, whereas the bottom part to those with overshoot. The entries of Table 12 are the initial stellar mass, the age at the end of the second dredge-up, the fractionary mass $Q_{\rm conv}$ of the layer reached by the external convection at its maximum penetration, and the abundances (by mass) of several elements, i.e. ^{1}H, ^{4}He, ^{12}C, ^{13}C, ^{14}N and ^{16}O. As already said, of the tabulated models only the $4M_\odot$, $5M_\odot$ and $6M_\odot$ stars experience the second dredge-up with consequent significant variations in the surface abundances. We like to point out the following consideratons for the case of models with overshoot, as a similar analysis can be made easily for the semiconvective models, we notice the following. Since the amount of helium which is brought into the external convective zone increases with the star mass, the largest variations in the surface chemical abundances with respect to those induced by the first dredge-up are expected to occur for the $6M_\odot$ star, whereas very little variations are seen for the $4M_\odot$ model. In the $6M_\odot$ star we notice a decrease of about 12% in ^{1}H, of about 15% in ^{12}C, and of about 13% in ^{16}O. Similarly, an increase of about 23% and 34% is seen in the abundance of ^{4}He and ^{14}N, respectively.

6.5. *Models for a $5M_\odot$ star with the new radiative opacities*

Figure 7 shows the evolutionary path in the HRD of the $5M_\odot$ star (chemical composition $Z = 0.008$ and $Y = 0.25$) calculated with the new radiative opacity of Iglesias & Rogers (1991a,b) and both core and envelope overshoot according to the assumption made in Sect. 3. In the same figure we also show the case with the standard LAOL of Huebner et al. (1977) for comparison. Figure 8 shows the corresponding fractionary mass of the convective core as function of the age during the central H- and He-burning phases. Similar calculations are made for the $5M_\odot$ star with metallicity $Z = 0.02$ and $Y = 0.28$. The results are shown in Figs. 9 (path in the HRD) and 10 (time variation of the convective core). The particular set of opacity used in these models includes the revision of the iron abundance made by Grevesse (1991). The new abundance of iron is about 30% lower than in the Anders & Grevesse (1989) mixture adopted in previous opacity calculations by the same authors (see Iglesias et al. 1992 for more details). As expected, with the new opacity the model stars run at slightly lower luminosity (the effect is more pronounced for the high metallicity star), possess a slightly bigger convective core (the effect is almost independent of the metal content), and live longer than with the old opacity of Huebner et al. (1977). Finally, we like to draw attention to the fact that, while the absolute core H- and He-

burning lifetimes do depend on the opacity in use, the ratio τ_{He}/τ_H is almost insensitive to it. Specifically, for the $Z = 0.008$ star the ratio varies from 0.08 (LAOL) to 0.10 with the new opacity (OPAL), whereas for the case with $Z = 0.02$ the ratio increases from 0.09 to about 0.13. This behaviour of the τ_{He}/τ_H ratio with the opacity source is particularly important, as it implies that the relative proportions of main sequence to post main sequence stars are by far more related to the mixing scheme than to opacity (compare the results presented in the previous section for the two mixing schemes). Finally the limited effect of the new opacity in the test models indicate that, despite the adoption of the old LAOL, the evolutionary results presented in this paper can be safely used to assess the effect of different mixing schemes and applied to many astrophysical problems. It goes without saying that the models we are going to present in forthcoming papers of this series will include the newest opacity sources.

7. Conclusions

In this paper we presented detailed numerical computations for stars in the mass range $0.6M_\odot$ to $100M_\odot$ and chemical composition $Y = 0.25$ and $Z = 0.008$. The models were calculated assuming two different schemes for convective mixing, i.e. either the classical Schwarzschild criterion plus semiconvection or convective overshoot. All evolutionary sequences were followed till the start of the TPAGB or C-ignition in the core as appropriate to the mass of the models. The evolution of chemical abundances of sixteen elements were followed in detail. Finally, the massive stars were evolved in presence of mass loss by stellar wind.

The efficiency of convective overshoot from the central cores and external envelopes was chosen in such a way that the evolutionary models fit the observational data (CMDs and LFs) of star clusters of any age and supergiant stars in the Milky Way and LMC. The mass loss rate for massive stars was taylored on the observational data for supergiant and Wolf-Rayet stars.

Owing to the homogeneity of these models as far as the physical input is concerned, the effect induced by the two mixing schemes can be singled out.

This paper is the first of a series aimed at providing complete grids of stellar models, accompanying isochrones, and integrated colors, as the starting point for accurate studies of star clusters of different ages and chemical compositions, and of the integrated properties of stellar aggregates of various complexity. Next in the series will be the sets with the following chemical compositions: (Y = 0.230 and Z = 0.0001), (Y = 0.230 and Z = 0.001), (Y = 0.240 and Z = 0.004), (Y = 0.280 and Z = 0.02 : the solar composition), and (Y = 0.475 and Z = 0.10), this latter particularly designed to tackle the problem of UV excess in elliptical galaxies.

The data presented in this paper are available from the authors on magnetic tape.

Acknowledgements. This work has been financially supported by the Italian Ministry of University, Scientific Research and Technology (MURST) and the Italian Space Agency (ASI).

References

Alexander D.R. 1975, ApJS 29, 363
Alexander D.R., Johnson H.R., Rympa R.L. 1983, ApJ 272, 773
Alongi M., Bertelli G., Bressan A., Chioso C. 1991, A&A 244, 95
Anders E., Grevesse N. 1989, Geochim. Cosmochim. Acta 53, 197
Andersen J., Nordstrom B., Clausen J.V. 1990, ApJ 363, L33
Anthony-Twarog B.J., Heim E.A., Twarog B.A., Caldwell N. 1991, AJ 102, 1056
Aparicio A., Bertelli G., Chiosi C., Garcia-Pelayo J.M. 1990, A&A 240, 262
Arnett W.D., Truran J.W. 1969, ApJ 157, 339
Baker N.H., Kuhfuss R. 1987, A&A 185, 117
Barbaro G., Pigatto L. 1984, A&A 136, 355
Batten A.H., Hill G., Lu W. 1991, PASP 103, 546
Becker S.A. 1981, A&AS 136, 355
Becker S.A., Mathews G.J. 1983, ApJ 270, 155
Bergbusch P.A., VandenBerg D.A., Infante L. 1991, AJ 101, 2102
Bertelli G., Bressan A., Chiosi C. 1984, A&A 130, 279
Bertelli G., Bressan A., Chiosi C. 1985, A&A 150, 33
Bertelli G., Bressan A., Chiosi C., Angerer K. 1986a, A&AS 66, 191
Bertelli G., Bressan A., Chiosi C., Angerer K. 1986b, in The Age of Stellar Clusters, ed. F. Caputo, Mem. Soc. Astron. Ital. 57, 427
Bertelli G., Bressan A., Chiosi C. 1992a, ApJ 392, 522
Bertelli G., Bressan A., Chiosi C., Mateo M., Wood P.R. 1992b, ApJ, in press
Bessel M.S., Brett J.M., Scholz M., Wood P.R. 1989, A&AS 77, 1
Bessel M.S., Brett J.M., Scholz M., Wood P.R. 1991, A&AS Erratum, 621
Bressan A. 1990, in Chemical and Dynamical Evolution of Galaxies, ed. F. Ferrini, P. Franco, F. Matteucci. Pisa: Giardina
Bressan A., Bertelli G., Chiosi C. 1981, A&A 102, 25
Bressan A., Bertelli G., Chiosi C. 1986, in The Age of Stellar Clusters, ed. F. Caputo, Mem. Soc. Astron. Ital. 57, 411
Brocato E., Buonanno R., Castellani V., Walker A.R. 1990, A&AS 71, 25
Brocato E., Castellani V. 1988, A&A 203, 293

Brunish W.M., Truran J.W. 1982a, ApJ 256, 247
Brunish W.M., Truran J.W. 1982b, ApJS 49, 447
Buzzoni A., Fusi-Pecci F., Buonanno R., Corsi C.E. 1983, A&A 128, 94
Canuto V., Mazzitelli I. 1991, ApJ 370, 295
Caputo F., Castellani V., Chieffi A., Pulone L., Tornambe' A. 1989, ApJ 340, 241
Carraro G. 1991, Master Thesis in Astronomy, Univ. of Padova, Italy
Carraro G., Chiosi C., Bertelli G., Bressan A. 1992, A&A submitted
Castellani V., Chieffi A., Straniero O. 1990, ApJS 74, 463
Castellani V., Chieffi A., Straniero O. 1992, ApJS 78, 517
Castellani V., Chieffi A., Pulone L., Tornambe' A. 1985, ApJ 296, 204
Castellani V., Giannone P., Renzini A. 1971a, Astr. Space Sci. 10, 340
Castellani V., Giannone P., Renzini A. 1971b, Astr. Space Sci. 10, 355
Cattaneo F., Brummel N.H., Toomre J., Lalagoli A., Hulburt N.E. 1991, ApJ 370, 282
Caughlan G.R., Fowler W.A., Harris M., Zimmermann B. 1985, Atomic Data Nucl. Data Tables 32, 197
Caughlan G.R., Fowler W.A. 1988, Atomic Data Nuc. Data Tables 40, 283
Chin C.W., Stothers R.B. 1991, ApJS 77, 299
Chiosi C. 1986, in Nucleosynthesis and Stellar Evolution, 16th Saas-Fee Course, ed. B. Hauck, A. Maeder & G. Meynet, Geneva Observatory, p. 199
Chiosi C. 1989, in The Use of Pulsating Stars in Fundamental Problems of Astronomy, ed. E.G. Schmidt, p. 19. Cambridge: Cambridge Univ. Press
Chiosi C., Bertelli G., Bressan A. 1992a, ARA&A 30, 235
Chiosi C., Bertelli G., Bressan A. 1992b, in Instabilities in Evolved Super and Hypergiants, ed. C. de Jager & H. Nieuwenhuijzen, Amsterdam: North Holland Publ., p. 145
Chiosi C., Bertelli A., Meylan G., Ortolani S. 1989a, A&AS 78, 89
Chiosi C., Bertelli G., Meylan G., Ortolani S. 1989b A&A 219, 167
Chiosi C., Maeder A. 1986, ARA&A 24, 239
Chiosi C., Summa C. 1970, Astr. Space Sci. 8, 478
Chiosi C., Wood P.R., Bertelli G., Bressan A., Mateo M. 1992c, ApJ 385, 205
Clausen J.V. 1991, A&A 246, 397
Cloutman L.D., Whitaker R.W. 1980, ApJ 237, 900
Cox A.N., Stewart J.N. 1970a, ApJS 19, 243
Cox A.N., Stewart J.N. 1970b, ApJS 19, 261
de Jager C., Nieuwenhuijzen H., van der Hucht K.A. 1988, A&AS 72, 259
Demarque P., Mengel J.C. 1972, ApJ 171, 583
Doom C. 1982a, A&A 116, 303
Doom C. 1982b, A&A 116, 308
Doom C. 1985, A&A 142, 143
Fagotto F. 1990, Master Thesis in Astronomy, Univ. of Padova, Italy
Fowler W.A., Caughlan G.R., Zimmermann B.A. 1975, AR&A 13, 69
Fusi-Pecci F., Ferraro F.R., Crocker D.A., Rood R.T., Buonanno R. 1990, A&A 238, 95
Gingold R.A. 1976, ApJ 204, 116
Graboske H.C., de Witt H.E., Grossman A.S., Cooper M.S. 1973, AJ 181, 457
Green E.M., Demarque P., King C.R. 1987, The Revised Yale Isochrones and Luminosity Functions, New Haven: Yale Univ. Observatory
Greggio L. 1984, in Stellar Nucléosynthesis, ed. C. Chiosi & A. Renzini, Dordrecht: Reidel, p. 137
Grevesse N. 1991, A&A 242, 488
Harm R., Schwarzschild M. 1966, ApJ 145, 496
Huebner W.F., Merts A.L., Magee N.H., Argo M.F. 1977, Los Alamos Scientific Laboratory Report LA-6760-M
Iben I. Jr. 1964, ApJ 141, 993
Iben I. Jr. 1991, ApJS 76, 55
Iben I. Jr., Renzini A. 1983, ARA&A 21, 271
Iben I. Jr., Renzini A. 1984, Physics Report 105, no. 6, 329
Iglesias C.A., Rogers F.J. 1991a, ApJ 371, 408
Iglesias C.A., Rogers F.J. 1991b, ApJ 371, L73
Iglesias C.A., Rogers F.J., Wilson B.G. 1987, ApJ 322, L45
Iglesias C.A., Rogers F.J., Wilson B.G. 1990, ApJ 360, 221
Iglesias C.A., Rogers F.J., Wilson B.G. 1992, ApJ submitted
Kettner K.U. et al. 1982, Phys. A-Atoms and Nuclei 308, 73
Kuhfuss R. 1986, A&A 160, 116
Langanke K., Koonin S.E. 1982, Nuclear Physics A410, 334
Langer N. 1986, A&A 164, 45
Langer N. 1989, A&A 210, 93
Lattanzio J.C. 1986, ApJ 311, 708
Lattanzio J.C. 1987, ApJ 313, L15
Lattanzio J.C. 1991, ApJS 76, 215
Lattanzio J.C., Vallenari A., Bertelli G., Chiosi C. 1991, A&A 340, 1991
Maeder A. 1975, A&A 40, 303
Maeder A. 1983, A&A 120, 113
Maeder A. 1990, A&AS 84, 139
Maeder A., Mermilliod J.C. 1981, A&A 93, 136
Maeder A., Meynet G. 1987, A&A 182, 243
Maeder A., Meynet G. 1988, A&AS 76, 411
Maeder A., Meynet G. 1989, A&A 210, 155
Maeder A., Meynet G. 1991, A&AS 89, 451
Matraka B., Wassermann C., Weigert A. 1982, A&A 107, 283
Mermilliod J.C., Maeder A. 1986, A&A 158, 45
Moskalik P., Buchler J.R., Marom A. 1991, ApJ 385, 685

Munakata H., Kohyama Y., Itoh N. 1985, ApJ 296, 197
Napiwotzki R., Schonberner D., Weidmann V. 1991, A&A 243, L5
Paczynski B. 1971, Acta Astron. 21, 417
Renzini A. 1977, in Advanced Stages of Stellar Evolution, ed. P. Bouvier & A. Maeder, Geneva Observatory, p. 151
Renzini A. 1987, A&A 188, 49
Renzini A., Fusi-Pecci F. 1988, ARA&A 26, 199
Renzini A., Voli M. 1981, A&A 94, 175
Robertson J.W., Faulkner D.J. 1972, ApJ 171, 309
Rogers F.J., Iglesias C.A. 1992, ApJ 79, 507
Roxburg I. 1978, A&A 65, 281
Roxburg I. 1989, A&A 211, 361
Russell S.C. & Bessel M.S. 1989, ApJS 70: 865
Saslow W.C., Schwarzschild M. 1965, ApJ 142, 1468
Schwarzschild M. 1970, QJRAS 11, 12
Shaviv G., Salpeter E.E. 1973, ApJ 184, 191
Stothers R.B. 1985, ApJ 298, 521
Stothers R.B. 1991, ApJ 383, 820
Stothers R.B., Chin C.W. 1981, ApJ 247, 1063
Stothers R.B., Chin C.W. 1990, ApJ 348, L21
Stothers R.B., Chin C.W. 1991a, ApJ 381, L67
Stothers R.B., Chin C.W. 1991b, ApJ 374, 288
Stothers R.B., Chin C.W. 1992, ApJ in press
Sweigart A.V., Demarque P. 1972, A&A 20, 445
Sweigart A.V., Greggio L., Renzini A. 1990, ApJ 364, 527
Sweigart A.V., Gross P.G. 1976, ApJS 32, 367
Sweigart A.V., Gross P.G. 1978, ApJS 36, 405
Vallenari A., Chiosi C., Bertelli G., Meylan G., Ortolani S. 1991, A&AS 87, 517
Vallenari A., Chiosi C., Bertelli G., Meylan G., Ortolani S. 1992, AJ 104, 1100
VandenBerg D.A. 1985, ApJS 58, 711
VandenBerg D.A. 1991, in The Formation and Evolution of Star Clusters, ed. K. Janes, ASPCS vol. 13, 183
Xiong D.R. 1985, A&A 150, 133
Xiong D.R. 1986, A&A 167, 239
Zahn J.-P. 1991, A&A 252, 179

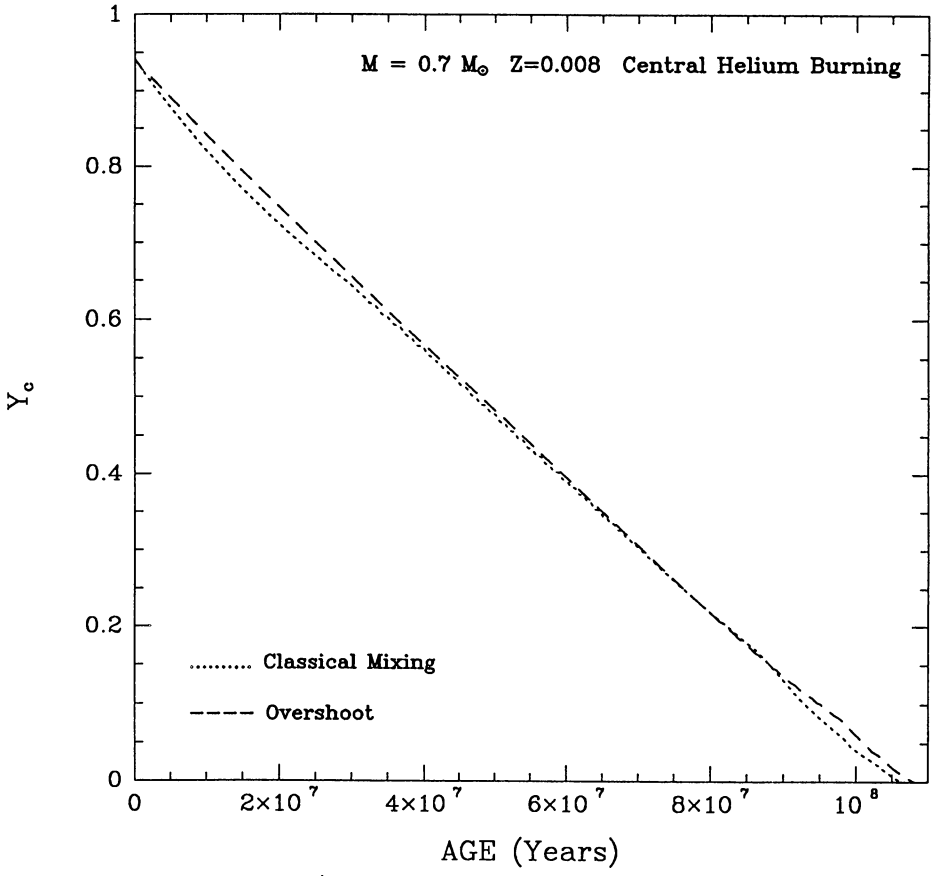

Fig. 1. The central He content Y_c as a function of the age (in years) for the model star of $0.6M_\odot$ calculated with both the semiconvective scheme (dotted line) and the overshoot scheme (dashed line). This figure shows that during the core He-burning phase the two mixing schemes lead to identical structures

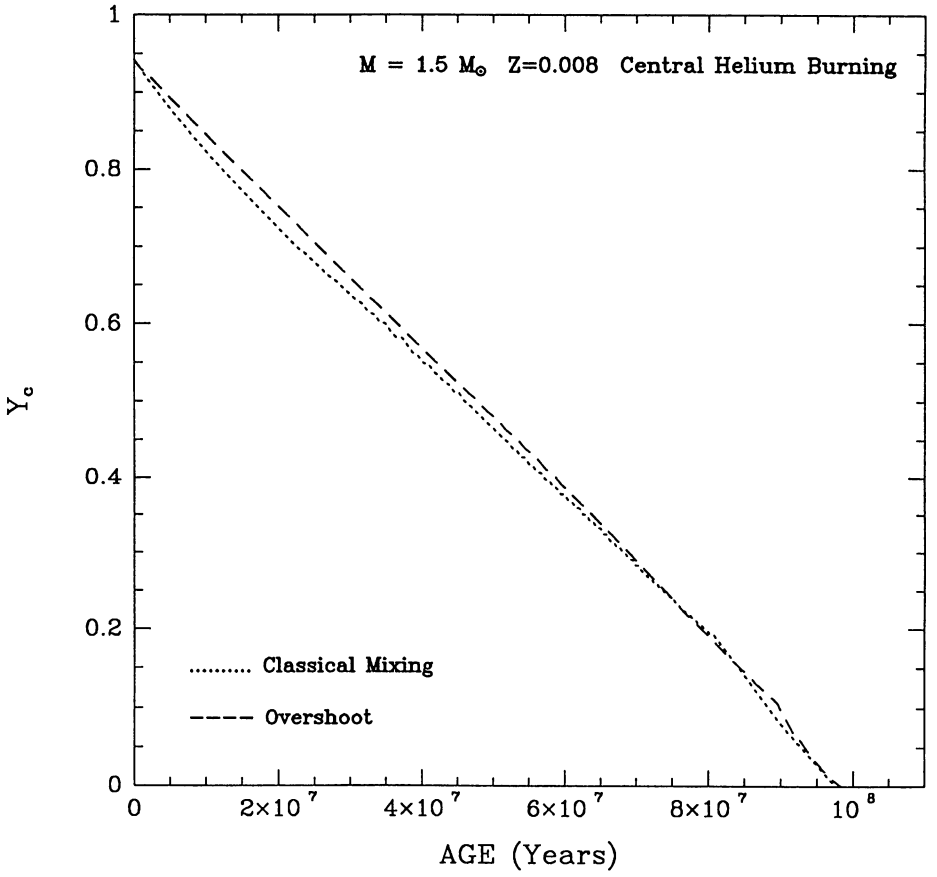

Fig. 2. The same as in Fig. 1 but for the model star of $1.5M_{\odot}$

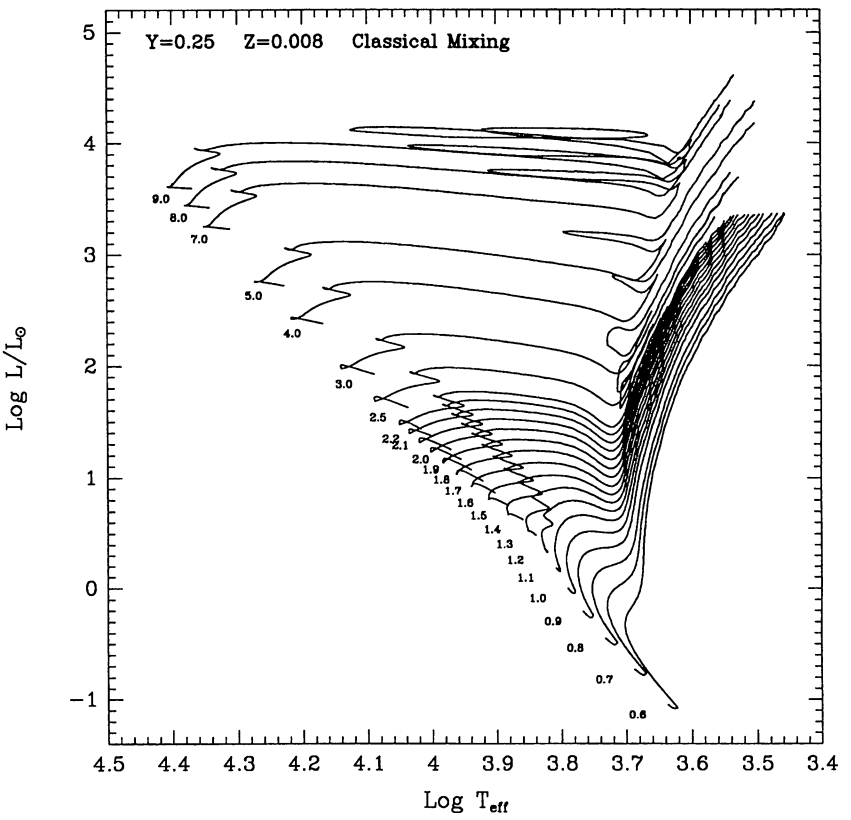

Fig. 3. The HRD of models calculated with the classical mixing scheme. The evolutionary tracks of stars lighter than $M_{\rm HeF}$ are shown up to the tip of the RGB, whereas those for the more massive stars extend up to the start of the TPAGB phase. Note the smooth transition from extended RGB to RGB *manque'* as the star mass approaches $M_{\rm HeF}$

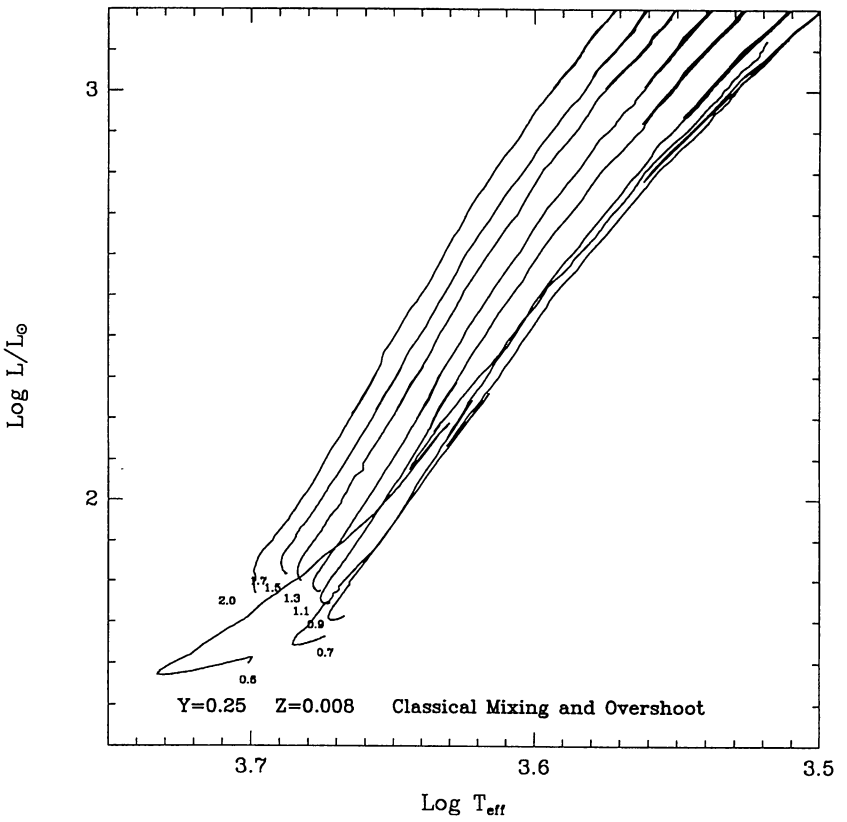

Fig. 4. The HRD for the core He-burning and EAGB phases of stars lighter than M_{HeF}

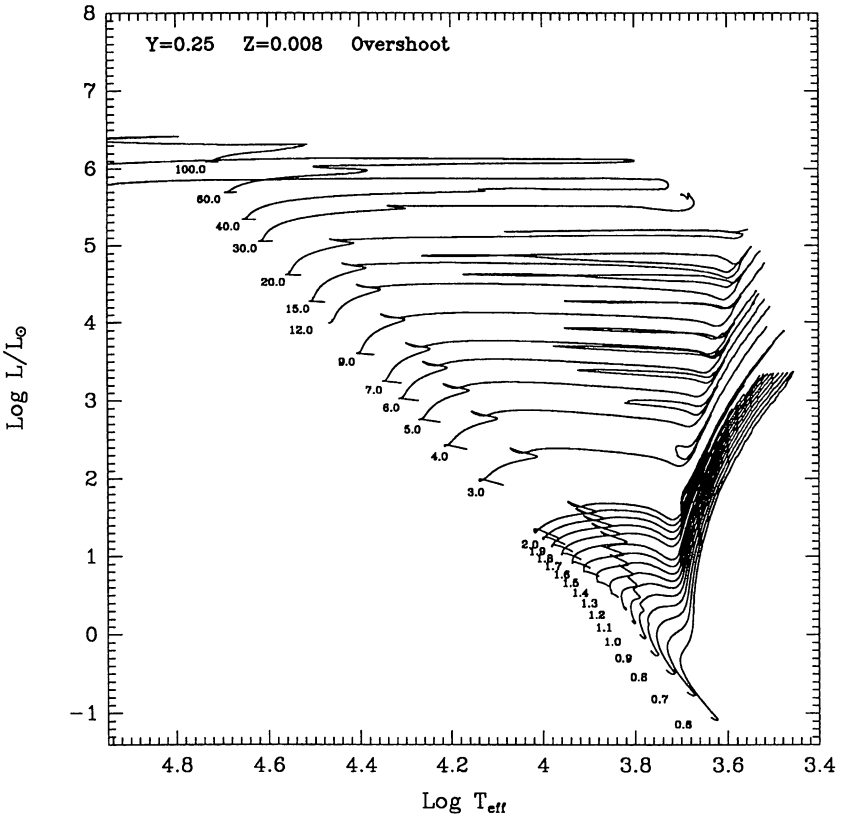

Fig. 5. The same as in Fig. 3 but for models calculated according to the overshoot scheme. This HRD also displays the evolutionary tracks of massive stars in occurrence of mass loss by stellar wind (see the text for more details)

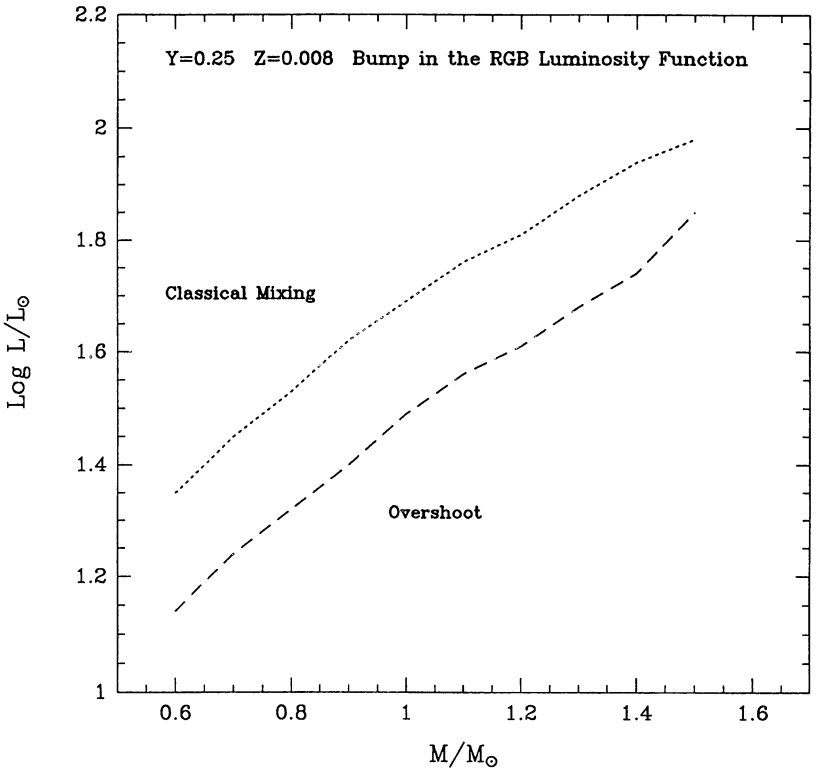

Fig. 6. The mean luminosity of the bump in the RGB luminosity function for models with overshoot (solid line) and models with classical mixing scheme (dashed line). Note the decrease in the luminosity induced by the deeper extension of the envelope convection in the case of overshoot models

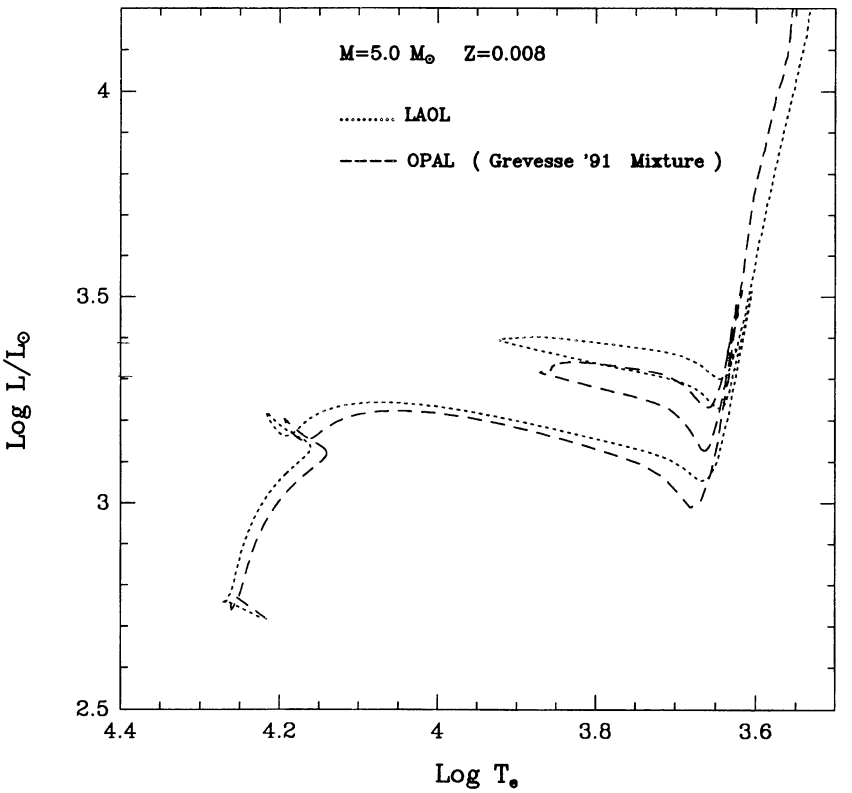

Fig. 7. The evolutionary path in the HRD of a $5M_{\odot}$ star with composition $Y = 0.25$ and $Z = 0.008$. These sequences are calculated with both core and envelope overshoot (see the text for details) and two sources of radiative opacity. LAOL stands for Huebner et al. (1977), while OPAL refers to Iglesias & Rogers (1991a,b)

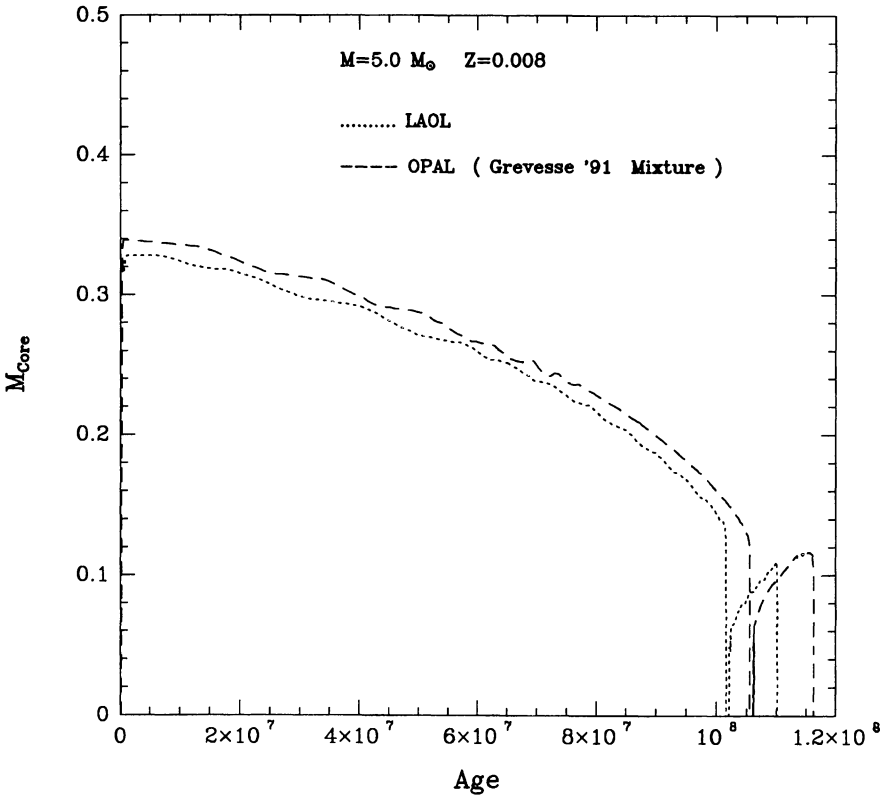

Fig. 8. The fractionary mass of the convective core as a function of the age during the central H- and He-burning phases of the $5M_{\odot}$ star shown in Fig. 7. The same notation as in Fig. 7 is adopted

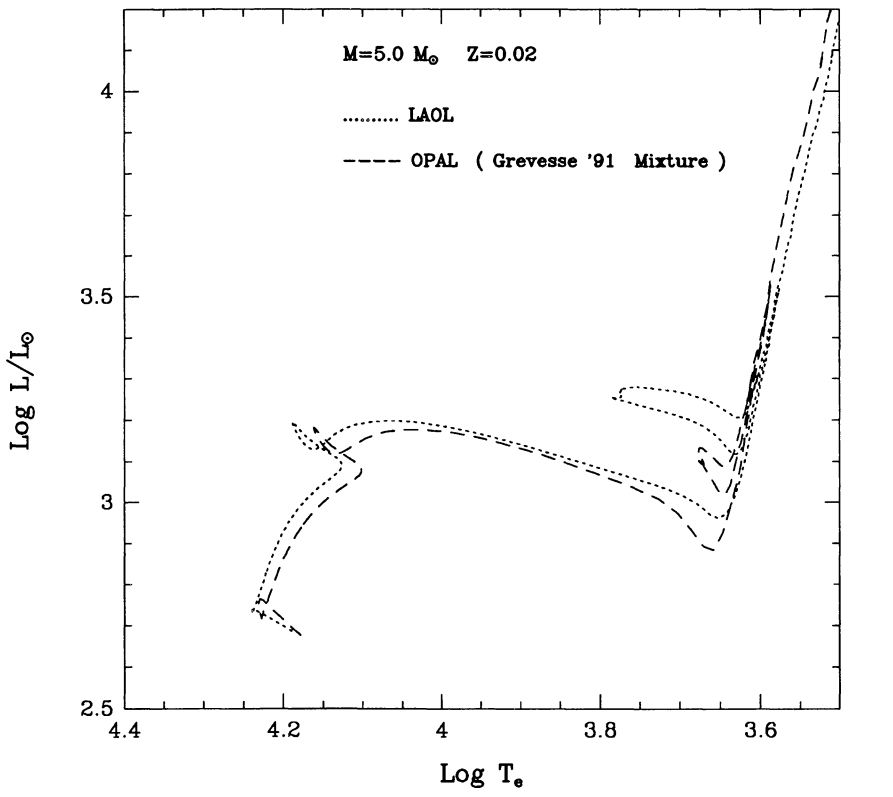

Fig. 9. The same as in Fig. 7 but for the $5M_{\odot}$ star with composition $Y = 0.28$ and $Z = 0.02$

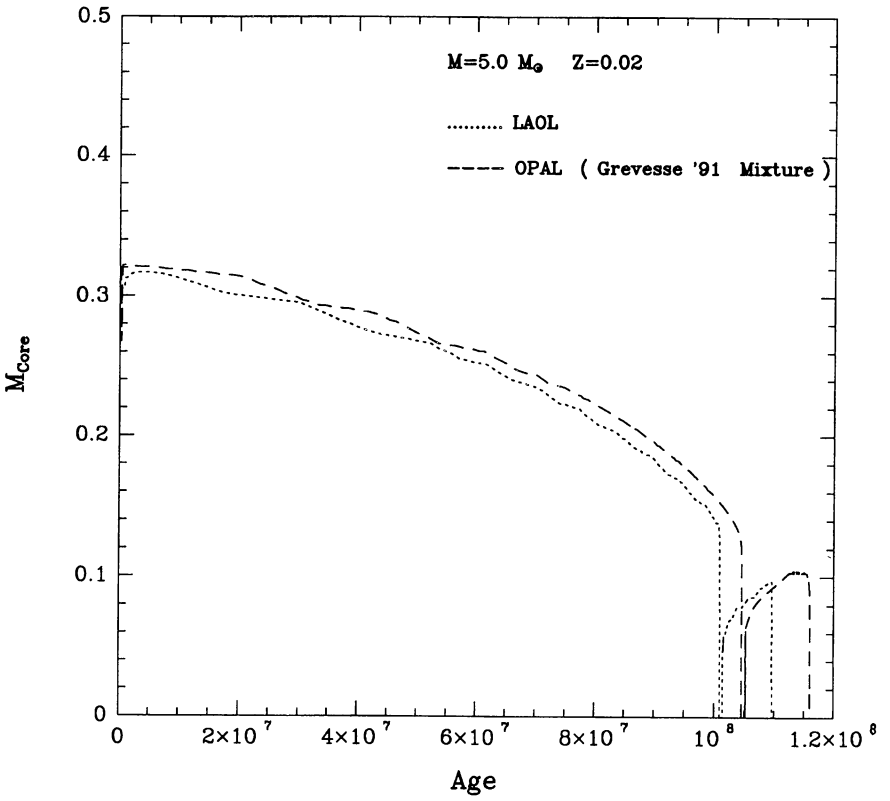

Fig. 10. The same as in Fig. 8 but for the $5M_{\odot}$ star with composition $Y = 0.28$ and $Z = 0.02$